INTERNATIONAL ATOMIC ENERGY AGENCY
UNITED NATIONS EDUCATIONAL, SCIENTIFIC AND CULTURAL ORGANIZATION

INTERNATIONAL CENTRE FOR THEORETICAL PHYSICS
34100 TRIESTE (ITALY) - P.O.B. 586 - MIRAMARE - STRADA COSTIERA 11 - TELEPHONES: 224281/2/3/4/5/6
CABLE: CENTRATOM - TELEX 46392 ICTP

SMR-30/ 30

WINTER COLLEGE ON ATOMIC AND MOLECULAR PHYSICS

26 January - 18 March 1977

SATURATED ABSORPTION LINE SHAPE: CALCULATION OF THE TRANSIT-TIME BROADENING BY A PERTURBATION APPROACH

(Taken from Phys.Rev.A, Vol.14, no.1, July 1976)

C.J. BORDÉ et al

Saturated absorption line shape: Calculation of the transit-time broadening by a perturbation approach

C. J. Bordé,* J. L. Hall,† C. V. Kunasz, and D. G. Hummer†
Joint Institute for Laboratory Astrophysics, University of Colorado and National Bureau of Standards, Boulder, Colorado 80302
(Received 24 November 1975)

We present a third-order perturbation calculation of line shapes in laser spectroscopy based on the density-matrix formalism. The new feature of this theory is the inclusion of the Gaussian spatial structure of the laser beams. We study the linewidth as a function of relaxation and transit times. A shift is found when the wave fronts are not flat. General line-shape formulas are given as well as approximate formulas valid in various domains.

I. INTRODUCTION

Since Lamb's first paper[1,2] on gas lasers, a number of theories of the Lamb dip (or of the saturated absorption line shape) have been developed. Each of these represents a new step toward a realistic calculation of the actual laboratory signal. Among other things, we now have a better understanding of the influence of a strong field, of the time pulsations or spatial modulations of the populations,[3-8] of the way collisions[9-11] shift the phase or change the velocity during the interaction, of the influence of level degeneracy, and of the Zeeman effect.[15-20] For molecular systems with long lifetimes, it was very soon recognized that the line shape would be dominated by the transit time of the molecules across the light beam.[21-25] Until now all detailed theories have dealt with plane waves and ignored the transverse geometry of the laser beam; they are therefore not applicable to the interesting low-pressure limit, to which one is naturally led in the pursuit of high resolution.

There are, in fact, several channels through which the geometry of the laser beam can influence the line shape:

(1) In the so-called free-flight regime, the molecules see a time-dependent field; thus the duration of coherent interaction is jointly controlled by the radiative lifetime, by collisions, and by the time of flight of the molecules across the beam.

(2) Even for high pressures or short lifetimes there is a space-dependent saturation parameter leading to a nonuniform saturation broadening.

(3) This space-dependent saturation will in turn result in a deformation of the beam geometry caused by differential absorption in the beam and the transversely nonuniform index of refraction. This last effect causes self-focusing or self-defocusing of the beam and induces asymmetry in the line.[26-28]

In this paper we shall consider only the problem defined in (1). Moreover, we limit ourselves here to a perturbation approach in which Lamb's third-order calculation is extended to Gaussian beams. We shall postpone to subsequent papers the extension of the theory to the strong-field case, where we will, in addition, include the recently resolved[29] recoil splitting.[30]

First, we review the basic equations: the density matrix equations for the molecular two-level system (Sec. II and Appendix A) and the electromagnetic equations for a Gaussian beam (Sec. III and Appendix B). Then (in Sec. IV) these equations are solved for the case of linear absorption spectroscopy. Section V develops the profile of the population changes in spatial and velocity coordinates. In Sec. VI we calculate the third-order polarization to obtain the saturated-absorption line shape. We present a plot of the resonance half-width as a function of the relaxation rate, and we also predict and study the shift which arises from wave-front curvature. In Sec. VII and Appendix C, a number of approximations are used to obtain simplified forms for the line shape, as well as useful asymptotic dependences of the line width and shift on lifetime and the beam geometry. The line-shape calculation for a frequency-modulated laser is sketched in Sec. VIII. For future application to the question of the accuracy of optical frequency standards, the second-order Doppler effect is included in some of our formulas.

II. DENSITY-MATRIX EQUATIONS FOR THE MOLECULAR SYSTEM

In this first paper we shall restrict ourselves to classical trajectories for molecules. We shall also assume, initially, that our equations are invariant under a Galilean transformation of the coordinates. Of the relativistic effects, the most important to our knowledge is the transverse Doppler effect, which can be introduced later into our equations. As there is a choice of frame of reference to describe the interaction, we shall try to take some care in specifying precisely the frame we use. Let $\vec{v}_R$ be the velocity of a given frame with respect to the laboratory and let $\vec{v}_M$ be the velocity of a molecule in that moving frame. We shall then deal with an elementary density operator

$$\rho(\vec{r},t,\vec{r}_0,t_0,\vec{v}_M,\alpha,\vec{v}_R)$$

for molecules created at time t_0 at location $\vec{r}_0$ in the state α. Because of the classical trajectory assumption, the position of the center of mass of such molecules is a function of time,

$$\vec{R}(t)=\vec{r}_0+\vec{v}_M(t-t_0)\,,$$

and ρ contains the implicit function

$$\delta(\vec{r}-\vec{R}(t))=\delta(\vec{r}-\vec{r}_0-\vec{v}_M(t-t_0))\,.$$

Thus our density matrix can be written

$$\rho(\vec{r},t,\vec{r}_0,t_0,\vec{v}_M,\alpha,\vec{v}_R)=\hat{\rho}(t,\vec{r}_0,t_0,\vec{v}_M,\alpha,\vec{v}_R)\delta(\vec{r}-\vec{r}_0-\vec{v}_M(t-t_0))\,.$$

We assume that the molecules keep their velocity $\vec{v}_M$ throughout their interaction with the light, and are lost to the coherent interaction if they suffer a velocity-changing collision or leave the illuminated region. For the purpose of this paper, the recoil splitting and the effect on the relaxation of velocity-changing collisions will be introduced in an *ad hoc* manner; in fact, both require a quantum-mechanical treatment of the translational motion.[11]

Among all possible reference systems, two are of special interest: the laboratory frame, and the frame at rest with respect to a class of molecules of given velocity (which we shall call the molecular frame). In the first case we shall write $\vec{v}_M=\vec{v}$ and $\vec{v}_R=0$; in the second case we write $\vec{v}_M=0$ and $\vec{v}_R=\vec{v}$.

We choose to connect the two descriptions by the Galilean transformation

$$\vec{r}=\vec{r}'+\vec{v}t'\,,\quad t=t'\,, \tag{1}$$

where primed quantities will refer to the molecular frame. In the molecular frame

$$\rho'(\vec{r}',t',\vec{r}_0',t_0',0,\alpha,\vec{v})$$

satisfies the equation

$$i\hbar\frac{\partial\rho'}{\partial t'}=[H_0+\tilde{V}',\rho']+i\hbar R\rho'\,, \tag{2}$$

where H_0 and $\tilde{V}'$ are, respectively, the Hamiltonian for the unperturbed isolated molecule and the Hamiltonian of interaction with the radiation field. All relaxation effects are included in the last term by the operator R acting on ρ' in the Liouville space. In this paper we shall assume the usual scalar electric-dipole interaction Hamiltonian

$$\tilde{V}'=-\tilde{\mu}\mathcal{E}'(\vec{r}',t')\,, \tag{3}$$

where $\mathcal{E}'(\vec{r}',t')$ is the electric field provided by the light source,

$$\mathcal{E}'(\vec{r}',t')=\mathcal{E}(\vec{r},t)=\mathcal{E}(\vec{r}'+\vec{v}t',t')\,. \tag{4}$$

In any other frame, Galilean invariance requires that Eq. (2) be written

$$i\hbar\left(\frac{\partial}{\partial t}+\vec{v}_M\cdot\vec{\nabla}\right)\rho=[H_0+\tilde{V},\rho]+i\hbar R\rho\,. \tag{5}$$

The hydrodynamic derivative in the left-hand side can also be justified from fully quantum-mechanical considerations as will be seen when we treat the recoil effect in a later paper.

It is usual to derive, from either Eq. (2) or Eq. (5), new equations for a more general density operator integrated over all possible formation conditions:

$$\rho(\vec{r},t,\vec{v}_M,\vec{v}_R)=\sum_\alpha\int_{-\infty}^{t}dt_0\int_{(\text{all space})}d^3r_0\lambda_\alpha(\vec{r}_0,t_0,\vec{v}_M,\vec{v}_R)\times\rho(\vec{r},t,\vec{r}_0,t_0,\vec{v}_M,\alpha,\vec{v}_R)\,, \tag{6}$$

where $\lambda_\alpha(\vec{r}_0,t_0,\vec{v}_M,\vec{v}_R)$ is the creation rate for molecules of velocity $\vec{v}_M$ in state α at $(\vec{r}_0,t_0)$. Calculating the hydrodynamic derivative of (6) and using Eq. (5) we have

$$\begin{aligned}\left(\frac{\partial}{\partial t}+\vec{v}_M\cdot\vec{\nabla}\right)\rho(\vec{r},t,\vec{v}_M,\vec{v}_R)&=\sum_\alpha\int_{(\text{all space})}d^3r_0\lambda_\alpha(\vec{r}_0,t,\vec{v}_M,\vec{v}_R)\rho(\vec{r},t,\vec{r}_0,t,\vec{v}_M,\alpha,\vec{v}_R)\\&+\sum_\alpha\int_{-\infty}^{t}dt_0\int_{(\text{all space})}d^3r_0\lambda_\alpha(\vec{r}_0,t_0,\vec{v}_M,\vec{v}_R)\left(\frac{\partial}{\partial t}+\vec{v}_M\cdot\vec{\nabla}\right)\rho(\vec{r},t,\vec{r}_0,t_0,\vec{v}_M,\alpha,\vec{v}_R)\\&=\sum_\alpha\lambda_\alpha(\vec{r},t,\vec{v}_M,\vec{v}_R)|\alpha\rangle\langle\alpha|\\&+\sum_\alpha\int_{-\infty}^{t}dt_0\int_{(\text{all space})}d^3r_0\lambda_\alpha(\vec{r}_0,t_0,\vec{v}_M,\vec{v}_R)\\&\times\left(\frac{1}{i\hbar}[H_0+\tilde{V},\rho(\vec{r},t,\vec{r}_0,t_0,\vec{v}_M,\alpha,\vec{v}_R)]+R\rho(\vec{r},t,\vec{r}_0,t_0,\vec{v}_M,\alpha,\vec{v}_R)\right),\end{aligned}$$

where the integration over $\vec{r}_0$ in the first term has been performed by making use of the boundary condition

$$\rho(\vec{r},t,\vec{r}_0,t,\vec{v}_M,\alpha,\vec{v}_R)=\delta(\vec{r}-\vec{r}_0)|\alpha\rangle\langle\alpha|\,. \tag{7}$$

Thus $\rho(\vec{r},t,\vec{v}_M,\vec{v}_R)$ satisfies the equation

$$i\hbar\left(\frac{\partial}{\partial t}+\vec{v}_M\cdot\vec{\nabla}\right)\rho=i\hbar\Lambda+[H_0+\tilde{V},\rho]+i\hbar R\rho\,, \tag{8}$$

where Λ is the operator $\sum_\alpha\lambda_\alpha(\vec{r},t,\vec{v}_M,\vec{v}_R)|\alpha\rangle\langle\alpha|$. By rewriting Λ as $-R\rho_0$ we obtain finally

$$i\hbar\left(\frac{\partial}{\partial t}+\vec{v}_M\cdot\vec{\nabla}\right)\rho=[H_0+\tilde{V},\rho]+i\hbar R(\rho-\rho_0)\,, \tag{9}$$

where ρ_0 can be interpreted as the unperturbed density operator.

To treat saturated absorption we shall consider only the usual nondegenerate two-level system with decay constants γ_a and γ_b for the populations and γ_{ab} for the optical dipole. The resonant frequency is $\omega_0=(E_a-E_b)/\hbar$ and the electric dipole matrix element is $\mu=\langle a|\tilde{\mu}|b\rangle$. Equation (9) then leads to a set of equations for the level populations and for the optical coherence.

In the laboratory frame ($\vec{v}_M=\vec{v}$, $\vec{v}_R=0$), for the level populations $n_\alpha(\vec{r},t,\vec{v})\equiv\rho_{\alpha\alpha}(\vec{r},t,\vec{v},0)$, $\alpha=a,b$, we obtain

$$\left(\frac{\partial}{\partial t}+\vec{v}\cdot\vec{\nabla}\right)n_a=-\gamma_a(n_a-n_a^{(0)})-i\frac{\mu\mathcal{E}(\vec{r},t)}{\hbar}(\rho_{ab}-\rho_{ab}^*)\,, \tag{10a}$$

$$\left(\frac{\partial}{\partial t}+\vec{v}\cdot\vec{\nabla}\right)n_b=-\gamma_b(n_b-n_b^{(0)})+i\frac{\mu\mathcal{E}(\vec{r},t)}{\hbar}(\rho_{ab}-\rho_{ab}^*)\,, \tag{10b}$$

and for the optical coherence $\rho_{ab}(\vec{r},t,\vec{v})\equiv\rho_{ab}(\vec{r},t,\vec{v},0)$, we have

$$\left(\frac{\partial}{\partial t}+\vec{v}\cdot\vec{\nabla}\right)\rho_{ab}=-i\omega_0\rho_{ab}-\gamma_{ab}\rho_{ab}-i\frac{\mu\mathcal{E}(\vec{r},t)}{\hbar}(n_a-n_b)\,. \tag{10c}$$

In the molecular frame ($\vec{v}_M=0$, $\vec{v}_R=\vec{v}$), for the level populations $n_\alpha'(\vec{r}',t',\vec{v})\equiv\rho_{\alpha\alpha}'(\vec{r}',t',0,\vec{v})$, we have

$$\frac{\partial n_a'}{\partial t'}=-\gamma_a(n_a'-n_a'^{(0)})-i\frac{\mu\mathcal{E}(\vec{r}'+\vec{v}t',t')}{\hbar}(\rho_{ab}'-\rho_{ab}'^*)\,, \tag{11a}$$

$$\frac{\partial n_b'}{\partial t'}=-\gamma_b(n_b'-n_b'^{(0)})+i\frac{\mu\mathcal{E}(\vec{r}'+\vec{v}t',t')}{\hbar}(\rho_{ab}'-\rho_{ab}'^*)\,, \tag{11b}$$

and for the optical coherence,

$$\frac{\partial\rho_{ab}'}{\partial t'}=-i\omega_0\rho_{ab}'-\gamma_{ab}\rho_{ab}'-i\frac{\mu\mathcal{E}(\vec{r}'+\vec{v}t',t')}{\hbar}(n_a'-n_b')\,. \tag{11c}$$

For both frames we have assumed a diagonal density matrix when there is no radiation. The equilibrium populations are, respectively, denoted by $n_\alpha^{(0)}$ and $n_\alpha'^{(0)}$ and, in general, depend on space and time, as well as velocity.

We note the following transformation laws between the frames:

$$\begin{aligned}n_\alpha'(\vec{r}',t',\vec{v})&=n_\alpha(\vec{r},t,\vec{v})=n_\alpha(\vec{r}'+\vec{v}t',t',\vec{v})\\&=n_\alpha'(\vec{r}-\vec{v}t,t,\vec{v})\,,\\\rho_{ab}'(\vec{r}',t',\vec{v})&=\rho_{ab}(\vec{r},t,\vec{v})=\rho_{ab}(\vec{r}'+\vec{v}t',t',\vec{v})\\&=\rho_{ab}'(\vec{r}-\vec{v}t,t,\vec{v})\,.\end{aligned} \tag{12}$$

In this paper we will be interested in the case of two quasimonochromatic waves counterpropagating along the z axis. We may take

$$\mathcal{E}(\vec{r},t)=A^+(\vec{r},t)e^{i(\omega t-kz)}+A^-(\vec{r},t)e^{i(\omega t+kz)}+\text{c.c.}\,, \tag{13}$$

where A^+ and A^- are slowly varying functions of x, y, z, and t which will later be defined more precisely. Since it is well known that Eqs. (10) [or (11)] cannot be solved analytically for the general case, we shall consider approximate solutions based on series expansions or numerical quadratures.

We will expect solutions of the form

$$\begin{aligned}n_\alpha&=\sum_{p=-\infty}^{+\infty}n_{\alpha,2p}\,e^{2ipkz}\,,\\\rho_{ab}&=\sum_{p=-\infty}^{\infty}\rho_{ab,2p+1}\,e^{(2p+1)ikz}\,e^{-i\omega t}\,,\end{aligned} \tag{14}$$

where nonresonant terms have been omitted and where the Fourier coefficients $n_{\alpha,2p}$ and $\rho_{ab,2p+1}$ are slowly varying functions of $\vec{r},t$. A corresponding expression in the molecular rest frame has the form

$$\begin{aligned}n_\alpha'&=\sum_{p=-\infty}^{\infty}n_{\alpha,2p}'\exp[2ipk(z'+v_zt')]\,,\\\rho_{ab}'&=\sum_{p=-\infty}^{\infty}\rho_{ab,2p+1}'\exp[(2p+1)ik(z'+v_zt')]e^{-i\omega t'}\,.\end{aligned} \tag{15}$$

These Fourier amplitudes satisfy coupled differential equations derived from Eq. (10),

$$\left(\frac{\partial}{\partial t}+\vec{v}\cdot\vec{\nabla}\right)n_{\alpha,2p}=-(2ipkv_z+\gamma_\alpha)(n_{\alpha,2p}-n_\alpha^{(0)}\delta_{p0})+\epsilon_\alpha\frac{\mu}{i\hbar}(A^+\rho_{ab,2p+1}+A^-\rho_{ab,2p-1}-A^{+*}\rho^*_{ab,-2p+1}-A^{-*}\rho^*_{ab,-2p-1}), \tag{16a}$$

$$\left(\frac{\partial}{\partial t}+\vec{v}\cdot\vec{\nabla}\right)\rho_{ab,2p+1}=-\{i[\omega_0-\omega+(2p+1)kv_z]+\gamma_{ab}\}\rho_{ab,2p+1}+\frac{\mu A^{+*}}{i\hbar}(n_{a,2p}-n_{b,2p})+\frac{\mu A^{-*}}{i\hbar}(n_{a,2p+2}-n_{b,2p+2}), \tag{16b}$$

where $\epsilon_a=1$ and $\epsilon_b=-1$. Corresponding equations hold in the molecular frame.

These equations can be directly solved numerically using a predictor-corrector method such as Hamming's or a similar technique designed to handle such equations. Solutions obtained using this technique will be presented in a later paper.[31]

Here we will examine solutions based on series expansions in ascending powers of the laser perturbation. This approach is naturally suggested by the implicit nature of the equations (10) and their integral form given in Appendix A. We take

$$n_\alpha=\sum_{q=0}^{\infty}n_\alpha^{(q)}\quad\text{and}\quad\rho_{ab}=\sum_{q=1}^{\infty}\rho_{ab}^{(q)}, \tag{17}$$

where q refers to the order of the interaction and is even for n_α and odd for ρ_{ab}.

For each perturbation order there are a number of Fourier components. This leads to the following double series:

$$n_\alpha=\sum_{q=0}^{\infty}n_\alpha^{(q)}=\sum_{q=0}^{\infty}\sum_{2p=-q}^{+q}n_{\alpha,2p}^{(q)}e^{2ipkz},\quad\alpha=a,b,$$

$$\rho_{ab}=\sum_{q=1}^{\infty}\rho_{ab}^{(q)}=\sum_{q=1}^{\infty}\sum_{2p+1=-q}^{+q}\rho_{ab,2p+1}^{(q)}e^{(2p+1)ikz}e^{-i\omega t}, \tag{18}$$

where $n_{\alpha,2p}^{(q)}$ and $\rho_{ab,2p+1}^{(q)}$ are slowly varying functions of x, y, and z.

In the molecular frame we have the corresponding expansions

$$n'_\alpha=\sum_{q=0}^{\infty}n_\alpha'^{(q)}=\sum_{q=0}^{\infty}\sum_{2p=-q}^{+q}n'^{(q)}_{\alpha,2p}\exp[2ipk(z'+v_zt')],$$

$$\rho'_{ab}=\sum_{q=1}^{\infty}\rho'^{(q)}_{ab}=\sum_{q=1}^{\infty}\sum_{2p+1=-q}^{+q}\rho'^{(q)}_{ab,2p+1}\times\exp[(2p+1)ik(z'+v_zt')]e^{-i\omega t'}. \tag{19}$$

With these expansions, Eqs. (16) can be rewritten for each perturbation order.

III. ELECTROMAGNETIC EQUATIONS

In this paper we are interested in calculating either an absorption coefficient for a light beam or a fluorescence signal from a molecular level. Both quantities are proportional to the power absorbed from the light by the molecules. Introducing the complex Poynting vector

$$\vec{R}=\vec{E}\times\vec{B}^*/2\mu_0,$$

we can write the energy balance equation for the volume V within the surface S as

$$\operatorname{Re}\int_S\vec{R}\cdot d\vec{S}=-\frac{\partial}{\partial t}\int_V\left(\epsilon_0\frac{\vec{E}\cdot\vec{E}^*}{4}+\frac{\vec{B}\cdot\vec{B}^*}{4\mu_0}\right)dV-\frac{\operatorname{Re}}{2}\int_V\vec{E}\cdot\frac{\partial\vec{P}^*}{\partial t}dV, \tag{20}$$

where complex representation of the vectors has been used, $\vec{\mathcal{E}}=\operatorname{Re}\vec{E}$ and so on.

The average power lost by the light is therefore

$$\overline{W}_{abs}=\frac{\operatorname{Re}}{2}\int_V\vec{E}\cdot\frac{\partial\vec{P}^*}{\partial t}dV, \tag{21}$$

which, for monochromatic light, becomes

$$\overline{W}_{abs}=\frac{\omega\operatorname{Im}}{2}\int_V\vec{E}\cdot\vec{P}^*dV. \tag{22}$$

The absorption coefficient for a field propagating along the optical axis z is defined by

$$\alpha(\omega,z)=\frac{1}{c\int\epsilon_0\frac{1}{2}\vec{E}\cdot\vec{E}^*dx\,dy}\frac{d\overline{W}_{abs}}{dz}=\frac{\omega}{c}\frac{\operatorname{Im}\int\vec{P}^*\cdot\vec{E}\,dx\,dy}{\int\epsilon_0\vec{E}\cdot\vec{E}^*dx\,dy}. \tag{23}$$

We now use a scalar formulation in which the electric field is linearly polarized, and we assume the rotating-wave approximation in which the polarization P is simply

$$P=2\mu\overline{\rho}^*_{ab},$$

where

$$\overline{\rho}_{ab}=\int\rho_{ab}(\vec{v})\,d^3v.$$

Multiplying the density matrix equations (10a) and (10b) by $\frac{1}{2}\hbar\omega$ and subtracting, we verify that

$$W_{abs}=-i\omega\mu\int(\rho_{ab}-\rho^*_{ab})\operatorname{Re}E\,dV\,d^3v=\int\operatorname{Re}E\frac{\partial\operatorname{Re}P}{\partial t}dV,$$

which has the time average given by (22).

We shall assume that the material medium affects the field only by changing the amplitude and the phase along the z axis. Since the transverse geometrical structure of the light beam is not affected, we regard it as being known exactly. As before, the field can be written as the sum of two counterpropagating waves,

$$E=[E_0^+(z)e^{i\phi^+(z)}U^++E_0^-(z)e^{i\phi^-(z)}U^-]e^{i\omega t}, \tag{24}$$

where

$$U^+=U_0^+(x,y,z)e^{-ikz}, \tag{25a}$$

$$U^-=U_0^-(x,y,z)e^{ikz}. \tag{25b}$$

In this paper we shall assume the usual TEM_{00} Gaussian mode for $U_0^\pm(x,y,z)$. Using the result of Appendix B we have

$$U_0^\pm(x,y,z)=L^\pm(z)\exp[-L^\pm(z)(x^2+y^2)/w_\pm^2]. \tag{26}$$

Here $L^\pm(z)$ are the complex Lorentzian functions

$$L^\pm(z)=\frac{1}{1\mp2i(z-z_\pm)/b_\pm}=\frac{w_\pm^2}{w_\pm^2(z)}\pm i\frac{b_\pm}{2R_\pm(z)}, \tag{27}$$

where $b_\pm$ is the confocal parameter for the beam having a waist at $z_\pm$ with a $1/e$ radius $w_\pm$ such that $b_\pm=kw_\pm^2$, and $w_\pm(z)$ and $R_\pm(z)$ are, respectively, the beam radius and the radius of curvature of the two waves at z. To recover the plane-wave limit, we see that when $b\to+\infty$, $L^\pm\to1$, $w_\pm(z)\to w_\pm\to\infty$ and $R_\pm(z)\to\infty$; thus $U_0^\pm\to1$. In evaluating Eq. (23) we must calculate the integrals

$$\overline{Q}^\pm(\omega,z)=\int Q^\pm(\omega,z,\vec{v})\,d^3v, \tag{28}$$

where

$$Q^\pm(\omega,z,\vec{v})=\frac{1}{n_0}\operatorname{Im}\left(e^{i\phi^\pm}\int\rho_{ab,\pm1}U_0^\pm dx\,dy\right)\times\left(\int U_0^\pm U_0^{\pm*}dx\,dy\right)^{-1}, \tag{29}$$

and we have eliminated the terms that vary rapidly with z. Here n_0 is a population-difference parameter which will be defined later. The quantities $Q^\pm$ have no dimension and appear as the fractional degree of excitation of the optical dipoles.

The absorption coefficients for the two waves are simply given in terms of $\overline{Q}^\pm(\omega,z)$ by

$$\alpha^\pm(\omega,z)=(\omega/c)n_0(2\mu/\epsilon_0E_0^\pm)\overline{Q}^\pm(\omega,z). \tag{30}$$

The corresponding effective nonlinear susceptibility $\chi''=\alpha^\pm\omega/c$ is the ratio of the energy stored per unit volume by n_0 dipoles times their fractional degree of excitation to the electromagnetic energy stored in the vacuum.

The other useful observable is the fluorescence signal from either level. For a slice dz we can obtain the value of this signal by integrating the density matrix equations (16) over transverse coordinates. By setting $p=0$ we obtain the average value

$$\gamma_\alpha^R\int\int dx\,dy\,(n_{\alpha,0}-n_\alpha^{(0)})=\epsilon_\alpha n_0\frac{\gamma_\alpha^R}{\gamma_\alpha}\frac{\mu E_0^+}{\hbar}Q^+(\omega,z,\vec{v})\int\int U_0^+U_0^{+*}dx\,dy+\epsilon_\alpha n_0\frac{\gamma_\alpha^R}{\gamma_\alpha}\frac{\mu E_0^-}{\hbar}Q^-(\omega,z,\vec{v})\int\int U_0^-U_0^{-*}dx\,dy. \tag{31}$$

We see that the fluorescence signal from level α has two contributions proportional to $\int Q^\pm(\omega,z,\vec{v})\,d^3v$ (where the factor $\gamma_\alpha^R/\gamma_\alpha$ gives the appropriate reduction in γ if nonradiative processes are important). The above equation also shows that in the perturbation approach, it is equivalent to calculate $\int\int n_{\alpha,0}^{(q)}dx\,dy$ or $Q^{(q-1)\pm}$ from $\rho_{ab}^{(q-1)}$.

The rest of this paper is devoted to the calculation of $\overline{Q}^\pm$ for various orders in the perturbation expansion of ρ_{ab}.

IV. LINEAR APPROXIMATION

In this approximation the populations keep their equilibrium values, which for simplicity we assume to be independent of space and time,

$$n_\alpha=n'_\alpha=n_\alpha^{(0)}=n_\alpha'^{(0)},\quad\alpha=a,b. \tag{32}$$

We introduce a normalized velocity distribution $F(\vec{v})$,

$$n_b^{(0)}-n_a^{(0)}=n_0F(\vec{v}).$$

The density matrix equations for the optical coherence may then be written

$$\left(\frac{\partial}{\partial t}+\vec{v}\cdot\vec{\nabla}\right)\rho_{ab}^{(1)}=-i\omega_0\rho_{ab}^{(1)}-\gamma_{ab}\rho_{ab}^{(1)}+i\frac{\mu}{\hbar}n_0F(\vec{v})\operatorname{Re}E(\vec{r},t) \tag{33}$$

in the laboratory frame and

$$\frac{\partial\rho_{ab}'^{(1)}}{\partial t'}=-i\omega_0\rho_{ab}'^{(1)}-\gamma_{ab}\rho_{ab}'^{(1)}+i\frac{\mu}{\hbar}n_0F(\vec{v})\operatorname{Re}E(\vec{r}'+\vec{v}t',t') \tag{33'}$$

in the molecular frame. Because of the linearity of the problem we can restrict ourselves to the calculation of $\overline{Q}^+$ by keeping only the corresponding part of the electromagnetic field in (24). To show the equivalence of the two forms (33) and (33′), we now solve the problem in both frames.

A. Calculation of the transit effect in the molecular frame

In the rotating-wave approximation, Eq. (33′) can be written

$$\frac{\partial\rho_{ab}'^{(1)}}{\partial t'}=-i\,\omega_0\rho_{ab}'^{(1)}-\gamma_{ab}\rho_{ab}'^{(1)}+\frac{i\mu}{2\hbar}n_0F(\vec v)E_0^+(z'+v_zt')e^{-i\phi^+(z'+v_zt')}\times U^{+*}(\vec r'+\vec v t')e^{-i\omega t'}. \tag{34}$$

With the boundary condition $\rho_{ab}'=0$ at $-\infty$, ρ_{ab}' is given by

$$\rho_{ab}'^{(1)}(\vec r',t',\vec v)=i\,\frac{\mu}{2\hbar}n_0F(\vec v)e^{-(\gamma_{ab}+i\omega_0)t'}\times\int_{-\infty}^{t'}dt''\,E_0^+(z'+v_zt'')e^{-i\phi^+(z'+v_zt'')}\times U^{+*}(\vec r'+\vec v t'')e^{[-i(\omega-\omega_0)+\gamma_{ab}]t''}. \tag{35}$$

With the new integration variable $\tau=t'-t''$, ρ_{ab}' takes the form

$$\rho_{ab}'^{(1)}(\vec r',t',\vec v)=i\,\frac{\mu}{2\hbar}n_0F(\vec v)e^{-i\omega t'}\times\int_0^{\infty}d\tau\,E_0^+(z'+v_zt'-v_z\tau)e^{-i\phi^+(z'+v_zt'-v_z\tau)}\times U^{+*}(\vec r'+\vec v t'-\vec v\tau)e^{-[i(\omega_0-\omega)+\gamma_{ab}]\tau}. \tag{36}$$

If the transformation laws in (12) are used, the above expression for ρ_{ab}' can be transformed into one for ρ_{ab} in the laboratory frame,

$$\rho_{ab}^{(1)}(\vec r,t,\vec v)=i\,\frac{\mu}{2\hbar}n_0F(\vec v)e^{-i\omega t}\times\int_0^{\infty}d\tau\,E_0^+(z-v_z\tau)\,e^{-i\phi^+(z-v_z\tau)}\times U^{+*}(\vec r-\vec v\tau)e^{[i(\omega-\omega_0)-\gamma_{ab}]\tau}. \tag{37}$$

At a given position z the integrals in (36) and (37) can be evaluated easily if we neglect all longitudinal transit-time effects (apart from the usual first-order Doppler effect), that is, if we neglect the presence of $v_z\tau$ in E_0^+, ϕ^+, and L^+. Then

$$\rho_{ab}^{(1)}(\vec r,t,\vec v)=i\,\frac{\mu}{4\hbar}n_0F(\vec v)E^*(\vec r,t)(\pi/a)^{1/2}W(i(b/\sqrt a)), \tag{38}$$

where

$$a=(L^{+*}/w_+^2)(v_x^2+v_y^2),$$

$$b=-(L^{+*}/w_+^2)(v_xx+v_yy)+\tfrac12\gamma_{ab}+\tfrac12 i(\omega_0-\omega+kv_z),$$

and $W(i(b/\sqrt a))=e^{b^2/a}\,\mathrm{erfc}(b/\sqrt a)$ is the probability function for complex arguments.[32] A similar expression can be written for $\rho_{ab}'^{(1)}$.

We see from (38) that the in-phase or out-of-phase components of the polarization are symmetric or antisymmetric with respect to $\omega_0-\omega+kv_z$ only if a and therefore L are real, that is, if there is no curvature of the wave front. Otherwise the phase between the field and the accumulated polarization changes as we proceed along x or y. The resulting shift can also be interpreted as the variation in the Doppler shift (owing to the curvature of the wave fronts) which changes as the molecules cross the beam.

For very large beam diameters ($b_+\to\infty$), $a\to0$ and the susceptibility is a complex Lorentzian,

$$\left(\frac{\pi}{a}\right)^{1/2}W\!\left(i\frac{b}{\sqrt a}\right)\to\frac{2}{\gamma_{ab}+i(\omega_0-\omega+kv_z)}.$$

As the calculation of $\tilde Q^+$ from the expression (38) leads to cumbersome integrals, we prefer to perform the integrations in a different order. We start with the projection of expression (37) on the Gaussian field, again neglecting the longitudinal transit-time effects,

$$Q^+(\omega,z,\vec v)=\Omega^+F(\vec v)\,\mathrm{Re}\int_0^{\infty}d\tau\,e^{[i(\omega-\omega_0)-\gamma_{ab}]\tau}\int\!\!\int dx\,dy\,U^+(\vec r)U^{+*}(\vec r-\vec v\tau)\left(\int\!\!\int dx\,dy\,U^+(\vec r)U^{+*}(\vec r)\right)^{-1}. \tag{39}$$

Here we have introduced the Rabi circular frequency $\Omega^+=\mu E_0^+/2\hbar$. Note that all effects of the absorber motion appear in the argument of $U^{+*}(\vec r-\vec v t)$, so that there is an intrinsic symmetry between the usual Doppler broadening owing to motion along the z axis and the line broadening owing to the transverse motion. The line shape for a given velocity class now appears as a Fourier transform involving the spatial autocorrelation function of the field. The autocorrelation

function is

$$\mathcal U^+(z,\vec v,\tau)=\int\!\!\int dx\,dy\,U^+(\vec r)U^{+*}(\vec r-\vec v\tau)=e^{-ikv_z\tau}\,\mathcal U_0^+(z,\vec v,\tau).$$

Here

$$\mathcal U_0^+(z,\vec v,\tau)\simeq\int\!\!\int dx\,dy\,U_0^+(x,y,z)\times U_0^{+*}(x-v_x\tau,y-v_y\tau,z)=\tfrac12\pi w_+^2\,e^{-v_r^2\tau^2/2w_+^2}, \tag{40}$$

where $v_r^2=v_x^2+v_y^2$. An important result is that this function, and therefore the line shape, is independent of z. This result is valid, of course, only in the approximation that transit-time effects along the z axis are negligible, which is the case for a soft (large optical f number) focus. Such effects result in a broadening of the order of $v_z/b_\pm$, which is much smaller than the transverse transit-time broadening as long as $b_\pm\gg w_\pm$, that is, as long as $w_\pm\gg\lambda$.

The correlation time $\tau_c^+\equiv w_+/v_r$ plays the role of an effective transit time across the beam. In a gas cell, the corresponding average broadening is of the order of

$$\Delta\omega=u/w_+\quad\text{or}\quad\Delta\nu=(1/2\pi)u/w_+,$$

where u is the most probable velocity. The last integral in $Q^+(\omega,z,\vec v)$ can be evaluated to obtain

$$Q^+(\omega,z,\vec v)=\Omega^+\tau_c^+F(\vec v)(\tfrac12\pi)^{1/2}\times\mathrm{Re}\{W((\tau_c^+/\sqrt2)(\omega-\omega_0-kv_z+i\gamma_{ab}))\}. \tag{41}$$

This result is symmetric with respect to the variable $\omega-\omega_0-kv_z$. This symmetry could have been seen in (39) by changing $\vec r$ into $\vec r+\vec v\tau$ and $\vec v$ into $-\vec v$.

B. Laboratory frame calculation

For the laboratory frame we have Eq. (33), which, in the rotating-wave approximation, is

$$\left(\frac{\partial}{\partial t}+\vec v\cdot\vec\nabla\right)\rho_{ab}^{(1)}=-i\,\omega_0\rho_{ab}^{(1)}-\gamma_{ab}\rho_{ab}^{(1)}+i\,n_0F(\vec v)\Omega^+e^{-i(\omega t+\phi^+)}U^{+*}(\vec r). \tag{42}$$

One may reduce this equation to a first-order ordinary differential equation by observing that

$$\frac{\partial\rho_{ab}^{(1)}}{\partial t}\to-i\,\omega\rho_{ab}^{(1)}, \tag{43}$$

for monochromatic light, and

$$\frac{\partial\rho_{ab}^{(1)}}{\partial z}\to ik\rho_{ab}^{(1)}, \tag{44}$$

for a single traveling wave, where we neglect the effects of changes in geometry along the z axis. If the light has a cylindrical symmetry, we may rotate the axes so that $v_{y_1}=0$, $v_{x_1}=v_r$, $v_{z_1}=v_z$. If $\vec r_1=(x_1,y_1,z_1)$, then Eq. (42) becomes

$$v_r\,\frac{\partial\rho_{ab}^{(1)}}{\partial x_1}=i(\omega-\omega_0-kv_z)\rho_{ab}^{(1)}-\gamma_{ab}\rho_{ab}^{(1)}+i\Omega^+n_0F(\vec v)e^{-i(\omega t+\phi^+)}U^{+*}(\vec r_1), \tag{45}$$

which has the solution

$$\rho_{ab}^{(1)}=i\Omega^+n_0F(\vec v_1)e^{-i(\omega t+\phi^+)}\times\exp\!\left([i(\omega-\omega_0-kv_z)-\gamma_{ab}]\frac{x_1}{v_r}\right)\times\frac{1}{v_r}\int_{-\infty}^{x_1}dx_1'\,U^{+*}(x_1',y_1,z)\times\exp\!\left(-[i(\omega-\omega_0-kv_z)-\gamma_{ab}]\frac{x_1'}{v_r}\right). \tag{46}$$

Introducing the new integration variable $\tau=(x_1-x_1')/v_r$, we have

$$\rho_{ab}^{(1)}(x_1,y_1,z,t,\vec v_1)=i\Omega^+n_0F(\vec v_1)e^{-i(\omega t+\phi^+)}\times\int_0^{\infty}d\tau\,U^{+*}(x_1-\tau v_r,y_1,z)e^{[i(\omega-\omega_0-kv_z)-\gamma_{ab}]\tau}, \tag{47}$$

which is seen to be completely equivalent to (37) if one takes into account the rotation of the axes and the negligibility of the axial transit-time effect. We shall use the above reduction of the hydrodynamic derivative to a single derivative when we treat the strong-field case.

Another way to solve the partial differential equation (33) is to use the Fourier transform of $\rho_{ab}^{(1)}$ with respect to x and y,

$$\rho_{ab}^{(1)}(\vec r,t,\vec v)=e^{i(kz-\omega t)}\int\!\!\int dk_x\,dk_y\,\rho_{ab}^{(1)}(k_x,k_y,z,\vec v)\times e^{i(k_xx+k_yy)}. \tag{48}$$

The Fourier expansion of the laser field is, from Appendix B,

$$E(\vec r,t)=E_0^+e^{i\phi^+}e^{i(\omega t-kz)}\frac{w_+^2}{4\pi}\times\int_{-\infty}^{+\infty}\int_{-\infty}^{+\infty}dk_x\,dk_y\times\exp[-(k_x^2+k_y^2)w_+^2/4L^+]\times e^{i(k_xx+k_yy)}. \tag{49}$$

If we again neglect the slow changes of E_0^+, ϕ^+, and L^+ with z, we get the algebraic relation

$$i(k_x v_x + k_y v_y)\rho_{ab}^{(1)}(k_x, k_y, z, \vec{v}) = \{i(\omega - \omega_0 - kv_z) - \gamma_{ab}\}\rho_{ab}^{(1)}(k_x, k_y, z, \vec{v}) \times \exp[-(k_x^2 + k_y^2)w_+^2/4L^{+*}] + i\Omega^+ n_0 F(\vec{v})e^{-i\phi^+}(w_+^2/4\pi) \quad (50)$$

Substituting (50) into (48), we obtain

$$\rho_{ab}^{(1)}(\vec{r}, t, \vec{v}) = i\Omega^+ n_0 F(\vec{v})e^{-i\phi^+}e^{i(kz-\omega t)}(w_+^2/4\pi) \times \int_{-\infty}^{+\infty}\int_{-\infty}^{+\infty} \frac{\exp[-(k_x^2+k_y^2)w_+^2/4L^{+*}]}{i(\omega_0 - \omega + kv_z + k_x v_x + k_y v_y) + \gamma_{ab}} \times e^{i(k_x x + k_y y)}\, dk_x\, dk_y. \quad (51)$$

This expression can be simplified by rotating the axes as before so that $v_{y_1} = 0$. Then

$$\rho_{ab}^{(1)}(x_1, y_1, z, t, \vec{v}_1) = i\Omega^+ n_0 F(\vec{v}_1)e^{-i\phi^+}e^{i(kz-\omega t)} \times \frac{w_+}{2\sqrt{\pi}}\sqrt{L^{+*}}\, e^{-L^{+*}(y_1^2/w_+^2)} \times \int_{-\infty}^{+\infty} \frac{\exp[-(w_+^2/4L^{+*})k_{x_1}^2 + ik_{x_1}x_1]}{i(\omega_0 - \omega + kv_z + k_{x_1}v_{x_1}) + \gamma_{ab}}\, dk_{x_1}. \quad (52)$$

After evaluating the last integral we obtain a result equivalent to (38); differences in form are due only to rotation of the axes. Projection of $\rho_{ab}^{(1)}$ onto the field U_0^+ [as in (39)] gives

$$Q^+(\omega, z, \vec{v}_1) = \mathrm{Re}\,\Omega^+ F(\vec{v}_1)\frac{(L^+L^{+*})^{1/2}}{\pi^{3/2}w_+}\int_{-\infty}^{+\infty}\exp\left(\frac{-(L^+ + L^{+*})y_1^2}{w_+^2}\right)dy_1 \times \int_{-\infty}^{+\infty} dx_1\left(\sqrt{L^+}\, e^{-L^+(x_1^2/w_+^2)}\int_{-\infty}^{+\infty} dk_{x_1}\frac{\exp\{-[(w_+^2/4L^{+*})k_{x_1}^2 + ik_{x_1}x_1]\}}{i(\omega_0 - \omega + kv_z + k_{x_1}v_r) + \gamma_{ab}}\right), \quad (53)$$

or

$$Q^+(\omega, z, \vec{v}_1) = \Omega^+ F(\vec{v}_1)(w_+/\sqrt{2\pi}) \times \mathrm{Re}\int_{-\infty}^{+\infty} dk_{x_1}\frac{\exp(-\frac{1}{2}w_+^2 k_{x_1}^2)}{i(\omega_0 - \omega + kv_z + k_{x_1}v_r) + \gamma_{ab}}. \quad (54)$$

The line shape now appears as a convolution of a wave-vector distribution with a Doppler-shifted Lorentzian. We obtain finally

$$Q^+(\omega, z, v_r, v_z) = \Omega^+\tau_c^+ F(\vec{v})(\tfrac{1}{2}\pi)^{1/2} \times \mathrm{Re}\{W((\tau_c^+/\sqrt{2})(\omega - \omega_0 - kv_z + i\gamma_{ab}))\}, \quad (55)$$

which is identical with (41).

It is interesting to note the parallel between the present case and the usual line-broadening case, where the profile is also expressed by the Voigt function $\mathrm{Re}W(z)$. Here we have a single velocity with a Gaussian distribution of k vectors rather than a single k vector with a Gaussian distribution of velocities.

With the Fourier expansion approach we see that the transit-time broadening appears as a residual first-order Doppler broadening associated with the distribution of wave vectors. After averaging over transverse velocities we therefore expect a broadening of the order

$$\Delta\omega = u\Delta k = u/w_+.$$

This equivalence between transit-time and residual Doppler broadening descriptions appears also in beam-foil spectroscopy. In that case the transit time is across the entrance slit and the Doppler effect is related to the direction of emission.

C. Velocity integration

For a gas sample in thermodynamic equilibrium the Maxwell-Boltzmann velocity distribution is appropriate, and is conveniently written as

$$F(\vec{v}) = F_1(v_z)F_2(v_r),$$

with

$$F_1(v_z) = (1/\sqrt{\pi}\,u)e^{-v_z^2/u^2}, \quad F_2(v_r) = (2v_r/u^2)e^{-v_r^2/u^2},$$

where

$$u = (2k_BT/M)^{1/2}$$

is the most probable velocity. Although one could perform the integration directly on $Q^+(\omega, z, \vec{v})$ as given by (41), we prefer to go back one step and use (39).

We first perform the integration over transverse velocities

$$\overline{Q}^{(1)+}(\omega, z) = \Omega^+\int_{-\infty}^{+\infty} dv_z\, F_1(v_z)\,\mathrm{Re}\int_0^{\infty} d\tau\, e^{[i(\omega-\omega_0-kv_z)-\gamma_{ab}]\tau}\int_0^{\infty} dv_r\, F_2(v_r)\mathfrak{U}_0^+(v_r, \tau)\left(\int\int dx\, dy\, U_0^+ U_0^{+*}\right)^{-1}$$

$$= \Omega^+\int_{-\infty}^{+\infty} dv_z\, F_1(v_z)\,\mathrm{Re}\int_0^{\infty}\frac{d\tau}{1 + (u^2\tau^2/2w_+^2)}e^{[i(\omega-\omega_0-kv_z)-\gamma_{ab}]\tau}.$$

A choice must now be made as to whether to integrate first over v_z or over τ. Both choices will be investigated, for if we start with the integration on τ we obtain as an interesting intermediate result the line shape for a particular v_z class of molecules,

$$\Omega^+\,\mathrm{Re}\int_0^{\infty}\frac{d\tau\exp[i(\omega - \omega_0 - kv_z) - \gamma_{ab}]\tau}{1 + (u^2\tau^2/2w_+^2)} = \Omega^+(w_+/\sqrt{2}\,u)\,\mathrm{Im}[E_1(-\zeta)e^{-\zeta} - E_1(\zeta)e^{\zeta}] \equiv G^+(\zeta), \quad (56)$$

where

$$\zeta = (\sqrt{2}\,w_+/u)(\omega - \omega_0 - kv_z + i\gamma_{ab}). \quad (57)$$

Here $E_1(\zeta) \equiv \int_\zeta^{\infty}(e^{-u}/u)\,du$ is the exponential integral function.[32,33]

This line shape could be observed in an atomic beam experiment under ideal collimation conditions. In saturation spectroscopy the v_z velocity is not defined more precisely than the value corresponding to the homogeneous line width. Still, this line profile for a single v_z group was found to be useful as an empirical line shape for fitting experimental saturation absorption peaks. Later we show that this line shape is indeed an approximation to the complete profile. For $\gamma_{ab} = 0$, we have simply

$$G^+(\zeta) = (\pi w_+/\sqrt{2}\,u)\Omega^+\exp[-|(\omega - \omega_0 - kv_z)(\sqrt{2}w_+/u)|], \quad (58)$$

for which the $1/e$ half-width is $\Delta\nu = (1/2\pi\sqrt{2})(u/w_+)$, whereas for large γ_{ab}, $G(\zeta)$ approaches a Lorentzian line shape of half-width γ_{ab}.

If, on the other hand, integration over v_z is performed first, we have

$$\overline{Q}^{(1)+}(\omega, z) = \Omega^+\frac{1}{\sqrt{\pi}\,u}\,\mathrm{Re}\int_0^{\infty}\frac{d\tau\exp[i(\omega - \omega_0) - \gamma_{ab}]\tau}{1 + (u^2\tau^2/2w_+^2)} \times \int_{-\infty}^{+\infty} dv_z\, e^{-v_z^2/u^2}e^{-ikv_z\tau}$$

$$= \Omega^+\,\mathrm{Re}\int_0^{\infty}\frac{d\tau\exp\{-k^2u^2\tau^2/4 + [i(\omega - \omega_0) - \gamma_{ab}]\tau\}}{1 + (u^2\tau^2/2w_+^2)}. \quad (59)$$

In the limit as $w_+ \to \infty$ we recognize that the last factor is the Voigt function,

$$\overline{Q}^{(1)+}(\omega, z) = \sqrt{\pi}\frac{\Omega^+}{ku}\,\mathrm{Re}W\left(\frac{\omega - \omega_0}{ku} + i\frac{\gamma_{ab}}{ku}\right). \quad (60)$$

If $\gamma_{ab} = 0$, we can also evaluate the integral in (59) to obtain

$$\overline{Q}^{(1)+}(\omega, z) = \Omega^+\frac{\pi}{4}\frac{\sqrt{2}\,w_+}{u}e^{k^2w_+^2/2} \times \left[e^{-(\sqrt{2}w_+/u)(\omega-\omega_0)}\mathrm{erfc}\left(\frac{kw_+}{\sqrt{2}} - \frac{\omega - \omega_0}{ku}\right) + e^{(\sqrt{2}w_+/u)(\omega-\omega_0)}\mathrm{erfc}\left(\frac{kw_+}{\sqrt{2}} + \frac{\omega - \omega_0}{ku}\right)\right].$$

As $b_+ \to \infty$, the transit effects should disappear. We have

$$\mathrm{erfc}\left(\frac{kw^+}{\sqrt{2}} \mp \frac{\omega - \omega_0}{ku}\right) \to \frac{\sqrt{2}}{\sqrt{\pi}\,kw^+}\exp\left[-\left(\frac{kw^+}{\sqrt{2}} \mp \frac{\omega - \omega_0}{ku}\right)^2\right]$$

and

$$\overline{Q}^{(1)+}(\omega, z) \to \Omega^+(\sqrt{\pi}/ku)e^{-[(\omega-\omega_0)/ku]^2};$$

that is, we obtain a Doppler profile. In the other limit, as $k \to 0$, we get $G^+(\zeta)$.

It is interesting to note that an identical calculation arises in the line shape theory of Doppler-free two-photon spectroscopy,[34] and leads to an equation similar to (59). The appropriate value for k will then be the difference between the moduli of the wave vectors of the two oppositely running waves. If these are equal, the resulting line shape is similar to that given by (56).

V. SECOND-ORDER APPROXIMATION

At this stage we are interested in calculating the shape of the hole burned in the ground-state population $n_b^{(2)}(\vec{r}, t, \vec{v})$ and of the population peak created in the excited state, $n_a^{(2)}(\vec{r}, t, \vec{v})$, under the influence of the two counterpropagating fields. In a first treatment we shall neglect the spatial population modulations at $\pm 2kz$ or temporal pulsations at $\pm 2kv_z t'$ and keep only the $n_{\alpha,0}^{(2)}$ terms in the expansion (18). It is indeed possible to show that the $n_{\alpha,\pm 2}^{(2)}$ terms do not contribute to the final result in a third-order theory in the limit of infinite Doppler width.

In the laboratory frame, we have from Eqs. (10)

$$\vec{v}\cdot\vec{\nabla}n_a^{(2)} = -\gamma_a n_a^{(2)} + (\mu/\hbar)\,\mathrm{Im}(E\rho_{ab}^{(1)}) \quad (61a)$$

and

$$\vec{v}\cdot\vec{\nabla}n_b^{(2)} = -\gamma_b n_b^{(2)} - (\mu/\hbar)\,\mathrm{Im}(E\rho_{ab}^{(1)}), \quad (61b)$$

where a steady state has been assumed for the populations.

In the molecular frame we use Eqs. (11a) and (11b) to obtain

$$\frac{\partial n'^{(2)}_{a,0}}{\partial t'} = -\gamma_a n'^{(2)}_{a,0} + \frac{\mu}{\hbar}\,\mathrm{Im}[E(\vec{r}\,'+\vec{v}t',t')\rho'^{(1)}_{ab}(\vec{r}\,',t',\vec{v})] \tag{62a}$$

and

$$\frac{\partial n'^{(2)}_{b,0}}{\partial t'} = -\gamma_b n'^{(2)}_{b,0} - \frac{\mu}{\hbar}\,\mathrm{Im}[E(\vec{r}\,'+\vec{v}t',t')\rho'^{(1)}_{ab}(\vec{r}\,',t',\vec{v})]. \tag{62b}$$

As these two sets of equations are equivalent, we shall solve only the molecular-frame system.

As both counterpropagating fields give similar terms, we may again drop one of them for the sake of simplicity. From (24) and (62) we have

$$\frac{\partial n'^{(2)}_{a,0}}{\partial t'} = -\gamma_a n'^{(2)}_{a,0} - i\frac{\mu}{2\hbar}E_0[e^{i\phi}e^{i\omega t'}U(\vec{r}\,'+\vec{v}t')\times\rho'^{(1)}_{ab}(\vec{r}\,',t',\vec{v}) - \text{c.c.}], \tag{63}$$

where $\rho'^{(1)}_{ab}(\vec{r}\,',t',\vec{v})$ is given by (36). Performing the integration and change of variable, we obtain

$$n'^{(2)}_{a,0}(\vec{r}\,',t',\vec{v}) = -i\frac{\mu E_0}{2\hbar}e^{i\phi}\int_0^\infty d\tau'\,U(\vec{r}\,'+\vec{v}t'-\vec{v}\tau')\rho'^{(1)}_{ab}(\vec{r}\,',t'-\tau',\vec{v})e^{-\gamma_a\tau'}e^{i\omega(t'-\tau')} + \text{c.c.}$$

$$= n_0F(\vec{v})\left(\frac{\mu E_0}{2\hbar}\right)^2\int_0^\infty d\tau'\,e^{-\gamma_a\tau'}U(\vec{r}\,'+\vec{v}t'-\vec{v}\tau')\int_0^\infty d\tau\,U^*(\vec{r}\,'+\vec{v}t'-\vec{v}\tau-\vec{v}\tau')$$

$$\times\exp\{-[i(\omega_0-\omega)+\gamma_{ab}]\tau\} + \text{c.c.} \tag{64}$$

The equivalent expression in the laboratory frame is obtained in a straightforward manner by replacing $\vec{r}\,'+\vec{v}t'$ with $\vec{r}$,

$$n^{(2)}_{a,0}(\vec{r},t,\vec{v}) = 2n_0F(\vec{v})\left(\frac{\mu E_0}{2\hbar}\right)^2\mathrm{Re}\int_0^\infty d\tau'\,e^{-\gamma_a\tau'}U(\vec{r}-\vec{v}\tau')\int_0^\infty d\tau\,U^*(\vec{r}-\vec{v}\tau-\vec{v}\tau')\exp\{-[i(\omega_0-\omega)+\gamma_{ab}]\tau\}. \tag{65}$$

The physical interpretation of this formula is as follows: The population peak at a given point x, y in space is the sum of all of the contributions which arrive at that point and have been created at some past time τ' along the path followed by the particular class of molecules with specified velocity components v_x, v_y. Each of these contributions is proportional to the intensity of the field at the corresponding point in space, $\vec{r}-\vec{v}\tau'$, and is weighted by the factor $e^{-\gamma_a\tau'}$, which accounts for the relaxation of the population peak. Substituting for the functions U and U^* and performing the integration over τ gives

$$n^{(2)}_{a,0}(\vec{r},t,\vec{v}) = 2n_0F(\vec{v})\left(\frac{\mu E_0}{2\hbar}\right)^2\int_0^\infty d\tau'\,L^*Le^{-(L+L^*)\frac{(x-v_x\tau')^2+(y-v_y\tau')^2}{w^2}}$$

$$\times e^{-\gamma_a\tau'}\,\mathrm{Re}\Big[\int_0^\infty d\tau\exp\left(-L^*\frac{v_x^2+v_y^2}{w^2}\tau^2\right)e^{2L^*\frac{v_x(x-v_x\tau')+v_y(y-v_y\tau')}{w^2}\tau}$$

$$\times\exp\{-[i(\omega_0-\omega\pm kv_z)+\gamma_{ab}]\tau\}\Big]$$

$$= n_0F(\vec{v})\left(\frac{\mu E_0}{2\hbar}\right)^2\int_0^\infty d\tau'\,LL^*e^{-(L+L^*)\frac{(x-v_x\tau')^2+(y-v_y\tau')^2}{w^2}}e^{-\gamma_a\tau'}\,\mathrm{Re}\left[\left(\frac{\pi}{a}\right)^{1/2}W\left(i\frac{b}{\sqrt{a}}\right)\right], \tag{66}$$

where now

$$a=(L^*/w^2)(v_x^2+v_y^2),$$

$$b'=\tfrac{1}{2}\gamma_{ab}+\tfrac{1}{2}i(\omega_0-\omega\pm kv_z)-(L^*/w^2)[v_x(x-v_x\tau')+v_y(y-v_y\tau')].$$

The peak (or the hole) at a given point in space is not symmetric with respect to $\omega_0-\omega\pm kv_z$ if there is a curvature of the wave front (L complex in b'). As noted before, this asymmetry arises from the Doppler shift associated with the inward/outward propagation of the light. Although it reverses as one goes transversely across the beam from $-\infty$ to $+\infty$, the situation is not all symmetric with respect to the beam center, because at a given point it depends on the accumulated history of the molecules that arrive there.

Although the local response function is not spatially symmetric, it is easy to check that the integral over space of $n^{(2)}_{a,0}(\vec{r},t,\vec{v})$ is a symmetric function of detuning. We can either calculate the integral of the expression (66) or directly integrate the equation (61a) over space to obtain

$$\iint n^{(2)\pm}_{a,0}\,dx\,dy = \frac{1}{\gamma_a}\frac{\mu E_0^\pm}{\hbar}\,\mathrm{Im}\left[e^{i\phi}\iint dx\,dy\,U_0^\pm\rho^{(1)}_{ab,\pm1}\right],$$

which is symmetric with respect to $\omega_0-\omega\pm kv_z$. This is consistent with the symmetry displayed by $Q^{(1)\pm}$ in Eq. (41), since the bracketed term is proportional to $Q^{(1)\pm}$.

VI. THIRD-ORDER APPROXIMATION

Using once more the equations for the nondiagonal element we are able to calculate $\rho^{(3)}_{ab,\pm1}$ and the shape of the saturated absorption signal. In the molecular frame we can write from Eq. (11c)

$$\frac{\partial\rho'^{(3)}_{ab}}{\partial t'} = -i\omega_0\rho'^{(3)}_{ab}-\gamma_{ab}\rho'^{(3)}_{ab}+i\frac{\mu}{2\hbar}[E_0^+e^{-i\phi^+}U_0^{+*}(\vec{r}\,'+\vec{v}t')e^{ik(z'+v_zt')}+E_0^-e^{-i\phi^-}U_0^{-*}(\vec{r}\,'+\vec{v}t')e^{-ik(z'+v_zt')}]e^{-i\omega t}(n_b'^{(2)}-n_a'^{(2)}). \tag{67}$$

Using Eq. (15) we get

$$\frac{\partial\rho'^{(3)}_{ab,\pm1}}{\partial t'} = -i(\omega_0-\omega\pm kv_z)\rho'^{(3)}_{ab,\pm1}-\gamma_{ab}\rho'^{(3)}_{ab,\pm1}+i(\mu/2\hbar)(n'^{(2)}_{b,0}-n'^{(2)}_{a,0})E_0^\pm e^{-i\phi^\pm}U_0^{\pm*}(\vec{r}\,'+\vec{v}t')$$

$$+i(\mu/2\hbar)(n'^{(2)}_{b,\pm2}-n'^{(2)}_{a,\pm2})E_0^\mp e^{-i\phi^\mp}U_0^{\mp*}. \tag{68}$$

We now drop the terms involving $n'^{(2)}_{\alpha,\pm2}$, because after integration over v_z they lead to negligible contributions when the Doppler width is very large compared to the saturated absorption peak width. For plane waves this is known as the rate-equation approximation. We therefore have

$$\rho'^{(3)}_{ab,\pm1} = i(\mu/2\hbar)E_0^\pm e^{-i\phi^\pm}\exp[-i(\omega_0-\omega\pm kv_z)t'-\gamma_{ab}t']$$

$$\times\int_{-\infty}^{t'}dt''\,[n'^{(2)}_{b,0}(\vec{r}\,',t'')-n'^{(2)}_{a,0}(\vec{r}\,',t'')]U_0^{\pm*}(\vec{r}\,'+\vec{v}t'')\exp\{[i(\omega_0-\omega\pm kv_z)+\gamma_{ab}]t''\}, \tag{69}$$

and by changing to $\tau''=t'-t''$, we find

$$\rho'^{(3)}_{ab,\pm1}(\vec{r}\,',t',\vec{v}) = i\Omega^\pm e^{-i\phi^\pm}\int_0^\infty d\tau''[n'^{(2)}_{b,0}(\vec{r}\,'+\vec{v}(t'-\tau''),t'-\tau'')-n'^{(2)}_{a,0}(\vec{r}\,'+\vec{v}(t'-\tau''),t'-\tau'')]$$

$$\times U_0^{\pm*}(\vec{r}\,'+\vec{v}(t'-\tau''))\exp\{-[i(\omega_0-\omega\pm kv_z)+\gamma_{ab}]\tau''\}. \tag{70}$$

In the laboratory frame these results have the form

$$\rho^{(3)}_{ab,\pm1}(\vec{r},t,\vec{v}) = i\Omega^\pm e^{-i\phi^\pm}\int_0^\infty d\tau''[n^{(2)}_{b,0}(\vec{r}-\vec{v}\tau'')-n^{(2)}_{a,0}(\vec{r}-\vec{v}\tau'')]U_0^{\pm*}(\vec{r}-\vec{v}\tau'')\exp\{-[i(\omega_0-\omega\pm kv_z)+\gamma_{ab}]\tau''\}, \tag{71}$$

and when the population changes are replaced by expression (65), we find

$$\rho^{(3)}_{ab,\pm1}(\vec{r},t,\vec{v}) = -i2\Omega^\pm e^{-i\phi^\pm}n_0F(\vec{v})$$

$$\times\int_0^\infty d\tau''U_0^{\pm*}(\vec{r}-\vec{v}\tau'')\exp\{-[i(\omega_0-\omega\pm kv_z)+\gamma_{ab}]\tau''\}$$

$$\times\Big((\Omega^+)^2\,\mathrm{Re}\int_0^\infty d\tau'(e^{-\gamma_b\tau'}+e^{-\gamma_a\tau'})U_0^+(\vec{r}-\vec{v}\tau'-\vec{v}\tau'')$$

$$\times\int_0^\infty d\tau\,U_0^{+*}(\vec{r}-\vec{v}\tau-\vec{v}\tau'-\vec{v}\tau'')\exp\{-[i(\omega_0-\omega+kv_z)+\gamma_{ab}]\tau\}$$

$$+(\Omega^-)^2\,\mathrm{Re}\int_0^\infty d\tau'(e^{-\gamma_b\tau'}+e^{-\gamma_a\tau'})U_0^-(\vec{r}-\vec{v}\tau'-\vec{v}\tau'')$$

$$\times\int_0^\infty d\tau\,U_0^{-*}(\vec{r}-\vec{v}\tau-\vec{v}\tau'-\vec{v}\tau'')\exp\{-[i(\omega_0-\omega-kv_z)+\gamma_{ab}]\tau\}\Big). \tag{72}$$

We now want to calculate the quantity

$$\bar{Q}^{(3)\pm}=\frac{1}{n_0}\int d^3v\,\mathrm{Im}\left(e^{i\phi\pm}\int \rho^{(3)}_{ab,\pm1}U_0^{\pm}dx\,dy\right)\Big/\int U_0^{\pm}U_0^{\pm *}\,dx\,dy. \tag{73}$$

In fact, to get the saturated absorption signal we need calculate only the change induced in each of these quantities by the presence of the other field,

$$\Delta\bar{Q}^{(3)\pm}=-\Omega^{\pm}(\Omega^{\mp})^2\int d^3v\,F(\vec{v})$$

$$\times\mathrm{Re}\bigg[\int\int dx\,dy\,U_0^{\pm}(\vec{r})\int_0^{\infty}d\tau''\,U_0^{\pm *}(\vec{r}-\vec{v}\tau'')\exp\{-[i(\omega_0-\omega\pm kv_z)+\gamma_{ab}]\tau''\}$$

$$\times\bigg(\int_0^{\infty}d\tau'\,U_0^{\mp}(\vec{r}-\vec{v}\tau'-\vec{v}\tau'')(e^{-\gamma_b\tau'}+e^{-\gamma_a\tau'})$$

$$\times\int_0^{\infty}d\tau\,U_0^{\mp *}(\vec{r}-\vec{v}\tau-\vec{v}\tau'-\vec{v}\tau'')\exp\{-[i(\omega_0-\omega\mp kv_z)+\gamma_{ab}]\tau\}$$

$$+\int_0^{\infty}d\tau'\,U_0^{\mp *}(\vec{r}-\vec{v}\tau'-\vec{v}\tau'')(e^{-\gamma_b\tau'}+e^{-\gamma_a\tau'})$$

$$\times\int_0^{\infty}d\tau\,U_0^{\mp}(\vec{r}-\vec{v}\tau-\vec{v}\tau'-\vec{v}\tau'')$$

$$\times\exp\{[i(\omega_0-\omega\mp kv_z)-\gamma_{ab}]\tau\}\bigg)\bigg]\Big/\int\int dx\,dy\,U_0^{\pm}U_0^{\pm *}. \tag{74}$$

In contrast to the linear case, it is more convenient to start with the integration on v_z,

$$\frac{1}{\sqrt{\pi}u}\int_{-\infty}^{+\infty}dv_z\exp\left(-\frac{v_z^2}{u^2}\right)\exp[\mp ik(\tau''\mp\tau)v_z]=\exp\{\tfrac{1}{4}[-k^2u^2(\tau''\mp\tau)^2]\}. \tag{75}$$

As was pointed out by Lamb,[2] in the infinite-Doppler-width limit the quantity

$$(ku/2\sqrt{\pi})\exp\{\tfrac{1}{4}[-k^2u^2(\tau''-\tau)^2]\}$$

acts like a δ function of $\tau''-\tau$, whereas $\exp\{\frac{1}{4}[-k^2u^2(\tau''+\tau)^2]\}$ gives a negligible contribution (as would have been the case for the spatial modulations of the populations $n^{(2)}_{a,\pm2}$ if we had kept them). The integration on τ'' therefore gives

$$\Delta\bar{Q}^{(3)\pm}=-\frac{2\sqrt{\pi}}{ku}\Omega^{\pm}(\Omega^{\mp})^2\int\int dv_x\,dv_y\,F_1(v_x)F_1(v_y)$$

$$\times\mathrm{Re}\bigg(\int\int dx\,dy\,U_0^{\pm}(\vec{r})\int_0^{\infty}d\tau\,U_0^{\pm *}(\vec{r}-\vec{v}_\perp\tau)\exp\{-2[i(\omega_0-\omega)+\gamma_{ab}]\tau\}$$

$$\times\int_0^{\infty}d\tau'\,U_0^{\mp}(\vec{r}-\vec{v}_\perp\tau'-\vec{v}_\perp\tau)(e^{-\gamma_b\tau'}+e^{-\gamma_a\tau'})$$

$$\times U_0^{\mp *}(\vec{r}-\vec{v}_\perp\tau'-2\vec{v}_\perp\tau)\bigg)\Big/\int\int dx\,dy\,U_0^{\pm}U_0^{\pm *}. \tag{76}$$

At this stage we write expressions such as $U_0(\vec{r}-\vec{v}_\perp\tau)$ to stand for $U_0(x-v_x\tau,y-v_y\tau,z)$, since we have already performed the integration on v_z; we have neglected the longitudinal transit-time effects that arise from terms such as $E_0(z-v_z\tau)$, $\phi(z-v_z\tau)$, or $L(z-v_z\tau)$.

For a Gaussian beam the integration could be performed separately on x and y, but it is simpler to recognize that the functions U_0 are cylindrically symmetrical and rotate coordinates so that $v_{y_1}=0$, $v_{x_1}=v_r$:

$$\Delta\bar{Q}^{(3)\pm}=-\frac{2\sqrt{\pi}}{ku}\Omega^{\pm}(\Omega^{\mp})^2\frac{2}{\pi w_\pm^2}L^{\pm}L^{\pm *}L^{\mp}L^{\mp *}$$

$$\times\int_{-\infty}^{+\infty}dy_1\exp\left[-\left(\frac{1}{w_\pm^2}(L^{\pm}+L^{\pm *})+\frac{1}{w_\mp^2}(L^{\mp}+L^{\mp *})\right)y_1^2\right]$$

$$\times\int_0^{\infty}dv_r\,F_2(v_r)\mathrm{Re}\bigg[\int_{-\infty}^{+\infty}dx_1\int_0^{\infty}d\tau\int_0^{\infty}d\tau'\exp\bigg(-L^{\pm}\frac{x_1^2}{w_\pm^2}-L^{\pm *}\frac{(x_1-v_r\tau)^2}{w_\pm^2}-L^{\mp}\frac{(x_1-v_r\tau'-v_r\tau)^2}{w_\mp^2}$$

$$-L^{\mp *}\frac{(x_1-v_r\tau'-2v_r\tau)^2}{w_\mp^2}\bigg)(e^{-\gamma_b\tau'}+e^{-\gamma_a\tau'})$$

$$\times\exp\{-2[i(\omega_0-\omega)+\gamma_{ab}]\tau\}\bigg]. \tag{77}$$

After performing the integration on x_1 and y_1 we obtain

$$\Delta\bar{Q}^{(3)\pm}=-\frac{2\sqrt{\pi}}{ku}\Omega^{\pm}(\Omega^{\mp})^2g_{\pm}\int_0^{\infty}dv_r\,F_2(v_r)\mathrm{Re}\int_0^{\infty}d\tau\int_0^{\infty}d\tau'\exp\{-v_r^2(A\tau'^2+2B_{\pm}\tau\tau'+C_{\pm}\tau^2)\}$$

$$\times(e^{-\gamma_b\tau'}+e^{-\gamma_a\tau'})\exp\{-2[i(\omega_0-\omega)+\gamma_{ab}]\tau\}, \tag{78}$$

with

$A=(l_++l_+^*)(l_-+l_-^*)/a=2/\{w_-^2(z)+w_+^2(z)\}$,

$B_{\pm}=(l_-l_++l_-^*l_+^*+2l_{\pm}l_{\mp}^*)/a$,

$C_{\pm}=[(l_{\mp}^*+l_-)(l_++l_-^*)+4l_{\pm}l_{\mp}^*]/a$,

where

$a=l_-+l_-^*+l_++l_+^*=2(1/w_+^2(z)+1/w_-^2(z))$,

$l_{\pm}=L^{\pm}/w_{\pm}^2$.

In addition we have introduced a geometrical factor

$$g_{\pm}=\int\int dx\,dy\,U_0^{\pm}(\vec{r})U_0^{\pm *}(\vec{r})U_0^{-}(\vec{r})U_0^{-*}(\vec{r})\Big/\int\int dx\,dy\,U_0^{\pm}(\vec{r})U_0^{\pm *}(\vec{r})=(2/aw_\pm^2)(L^+L^{+*}L^-L^{-*}).$$

For the matched Gaussian beams

$$g=\frac{1}{2}\;\frac{1}{1+4z^2/b^2};$$

for plane waves $g=1$. We next do the integration on τ' to obtain

$$\Delta\bar{Q}^{(3)\pm}=-\frac{2\sqrt{\pi}}{ku}\Omega^{\pm}(\Omega^{\mp})^2g_{\pm}\int_0^{\infty}dv_r\,\frac{F_2(v_r)}{v_r}\,\frac{1}{2}\left(\frac{\pi}{A}\right)^{1/2}\mathrm{Re}\int_0^{\infty}d\tau\exp\{-C_{\pm}v_r^2\tau^2-2[i(\omega_0-\omega)+\gamma_{ab}]\tau\}$$

$$\times\left[W\left(\frac{i}{\sqrt{A}}\left(\frac{\gamma_b}{2v_r}+B_{\pm}v_r\tau\right)\right)+W\left(\frac{i}{\sqrt{A}}\left(\frac{\gamma_a}{2v_r}+B_{\pm}v_r\tau\right)\right)\right]. \tag{79}$$

This we can rewrite as

$$\Delta\bar{Q}^{(3)\pm}=-\frac{\pi}{ku}\Omega^{\pm}(\Omega^{\mp})^2\frac{g_{\pm}}{\sqrt{A}}\int_0^{\infty}dv_r\,\frac{F_2(v_r)}{v_r}\mathrm{Re}\int_0^{\infty}d\tau\exp\left[-Dv_r^2\tau^2-\left(2\gamma_{ab}-\frac{B_{\pm}}{A}\gamma_b\right)\tau-2i(\omega_0-\omega)\tau+\frac{\gamma_b^2}{4Av_r^2}\right]$$

$$\times\mathrm{erfc}\frac{1}{\sqrt{A}}\left(B_{\pm}v_r\tau+\frac{\gamma_b}{2v_r}\right) \tag{80}$$

+ (same expression with γ_b replaced by γ_a), where

$$D=C_\pm-\frac{B_\pm^2}{A}=\frac{1}{2}\left(\frac{1}{w_+^2}+\frac{1}{w_-^2}\right)$$

is a real coefficient.

It is sometimes useful to know the contribution of different velocity groups; for this purpose one can perform a numerical integration over τ. In this case final results require further numerical integration over v_r. Later in this paper we reverse the order of integration and derive an analytic form for the velocity integral.

In the special cases, in which one or both beams are plane waves, analytic results can be given. If one beam has a very large confocal parameter ($b_\pm\to\infty$), then $w_\pm\to\pm\infty$ and $l_\pm\to 0$, and we find

$$\Delta Q^{(3)\pm}=-\frac{2\sqrt{\pi}}{ku}\Omega^\pm(\Omega^\mp)^2 g_\pm\left(\frac{1}{\gamma_a}+\frac{1}{\gamma_b}\right)\frac{2}{u^2}$$

$$\times\int_0^\infty dv_r\,v_r\exp\left(-\frac{v_r^2}{u^2}\right)$$

$$\times\mathrm{Re}\int_0^\infty \exp(-v_r^2\tau^2/2w_\pm^2)$$

$$\times\exp\{-2[i(\omega_0-\omega)+\gamma_{ab}]\tau\}d\tau\,.$$

Except for the factor of 2 in the exponent of the last integral, this is the same line shape as previously obtained in the case of the linear response of a given v_r velocity class, Eq. (56). This form can be anticipated by inspection of Eq. (76), where either $U_0^+(\vec{r})$ or $U_0^-(\vec{r})\to 1$.

If both beams are plane waves, beam-geometry effects disappear and we recover Lamb's result,

$$\Delta Q^{(3)\pm}=-\frac{\sqrt{\pi}}{ku}\Omega^\pm(\Omega^\mp)^2\left(\frac{1}{\gamma_a}+\frac{1}{\gamma_b}\right)$$

$$\times\mathrm{Re}\left(\frac{1}{i(\omega_0-\omega)+\gamma_{ab}}\right).$$

Before discussing the two integrations in Eq. (80) for the general case, we comment on the symmetry of the line shape. From (80) it can be seen that the line will be symmetric with respect to ω_0 only if $B_\pm$ is real. This is the case only if

$$L^+L^{-*}=L^{+*}L^-\,.$$

For matched beams, since $L^\pm\equiv L^{\mp*}$, this condition is fulfilled only for the waist where L is real. Otherwise $(L^+)^2\neq(L^{+*})^2$, and we expect an asymmetric peak if there is curvature of the wave fronts. This asymmetry is reversed if $B_\pm\to B_\pm^*$, that is, if the sign of the curvature of both beams is reversed or if the identification of the two beams is interchanged, i.e., $U^+\to U^-$, $U^-\to U^+$. We therefore expect a symmetric line shape only if the experiment has a plane of symmetry.

We could have come to the same conclusion by a close examination of expression (74), for by changing $\vec{r}_\perp$ into $\vec{r}_\perp+\vec{v}_\perp\tau+\vec{v}_\perp\tau'+\vec{v}_\perp\tau''$, $\omega_0-\omega$ into $\omega-\omega_0$, and $\vec{v}_\perp$ into $-\vec{v}_\perp$ in the complex conjugate of the first term, we see that it is invariant only if $U_0^\pm$ and $U_0^\mp$ can be interchanged.

To evaluate (80) we first need to calculate the line shape for a given class of transverse velocities, as given by

$$H^\pm(\omega-\omega_0,v_r)=(u\sqrt{D})^2\left(\frac{\pi}{A}\right)^{1/2}\frac{u}{v_r}F_2(v_r)e^{\gamma_b^2/4Av_r^2}$$

$$\times\int_0^\infty d\tau\exp(-Dv_r^2\tau^2-2\gamma_{ab}\tau)\left\{\mathrm{Re}\left[e^{(B_\pm/A)\gamma_b\tau}\,\mathrm{erfc}\frac{1}{\sqrt{A}}\left(B_\pm v_r\tau+\frac{\gamma_b}{2v_r}\right)\right]\cos 2(\omega_0-\omega)\tau\right.$$

$$\left.+\mathrm{Im}\left[e^{(B_\pm/A)\gamma_b\tau}\,\mathrm{erfc}\frac{1}{\sqrt{A}}\left(B_\pm v_r\tau+\frac{\gamma_b}{2v_r}\right)\right]\sin 2(\omega_0-\omega)\tau\right\}$$

$$+(\text{same integral with }\gamma_b\text{ replaced by }\gamma_a)\,. \tag{81}$$

This line shape is applicable without any further integration for saturated absorption experiments in a highly accelerated beam of atoms with a very narrow distribution in transverse velocities (but a flat one for axial velocities). In a beam of high-velocity neon atoms used for precise measurements of the transverse Doppler effect,[35] the distribution $F_2(v_r)$ was very nearly a δ function. For a gas in thermodynamic equilibrium

$$F_2(v_r)=(2/u^2)v_r\exp(-v_r^2/u^2)\,.$$

The integral over τ is evaluated numerically using an adaptive form of Simpson's rule. Then, for each choice of the laser beam and atomic parameters and for each value of the detuning we get a curve for H as a function of $\alpha=v_r/u$. Such a set of curves is shown in Fig. 1. Each of these curves gives the contribution of the various classes of

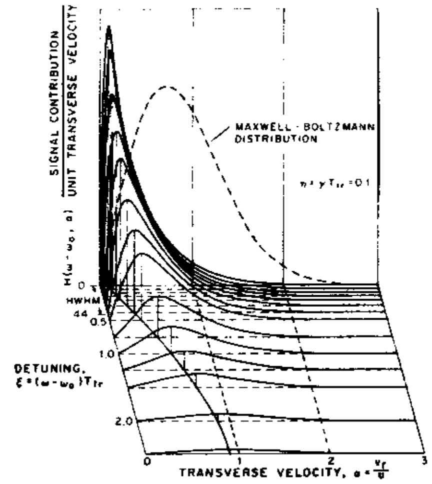

FIG. 1. Velocity selection effect in saturated absorption. The ordinate $H(\omega-\omega_0,\alpha)$ gives the contribution to the line shape of each transverse velocity class. These curves are calculated for the case of two matched beams at their waist and for an average transit time of $\frac{1}{10}$ of the lifetime.

transverse velocities to a particular point of the line shape.

If $b_\pm\to\infty$,

$$H=2(u\sqrt{D})^2uF_2(v_r)\left(\frac{1}{\gamma_b}+\frac{1}{\gamma_a}\right)$$

$$\times\mathrm{Re}\int_0^\infty\exp\{-2[\gamma_{ab}+i(\omega_0-\omega)]\tau\}\,d\tau$$

$$=(u\sqrt{D})^2uF_2(v_r)\left(\frac{1}{\gamma_b}+\frac{1}{\gamma_a}\right)\mathrm{Re}\left(\frac{1}{\gamma_{ab}+i(\omega_0-\omega)}\right).$$

This expression has the shape of the usual velocity distribution $uF_2(v_r)=2\alpha e^{-\alpha^2}$ with a maximum at $\alpha=\frac{1}{2}\sqrt{2}$.

In Fig. 1 we see that for a finite beam diameter this maximum is shifted towards smaller values of α. The physical interpretation of this shift is that because of the nonlinearity of saturated absorption, slow molecules spending more time in the beam make a relatively larger contribution. The relevant parameters are the ratios of the lifetimes $1/\gamma_a$, $1/\gamma_b$, and $1/\gamma_{ab}$ to the average transit time w/u. As these ratios increase, so do the relative contributions of the slow molecules, and the $H(\alpha)$ curves crowd toward the origin. This fact is of great importance in the evaluation of the second-order Doppler shift for optical frequency standards based on saturated absorption.

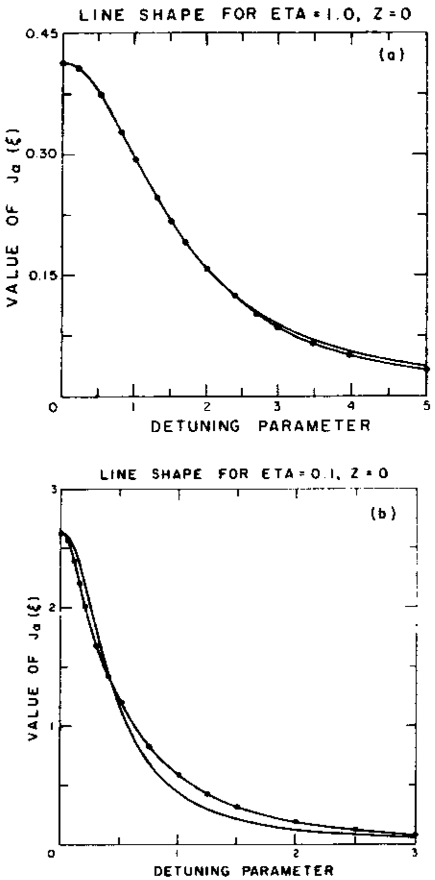

FIG. 2. Calculated line shapes $J_\alpha(\xi)$. (a) $\eta=\gamma T_{tr}=1.0$, (b) $\eta=0.1$. The curves without the ● symbol represent Lorentz functions with the same half-widths. The frequency detuning is in units of $T_{tr}^{-1}=u\sqrt{D}$. The function is symmetric in frequency.

For a given value of the detuning, the line shape is proportional to the area under the corresponding curve $H(\alpha)$, i.e.,

$$\Delta\bar{Q}^{(3)\pm}(\omega-\omega_0,z)=K^\pm\int_0^\infty H^\pm(\omega-\omega_0,\alpha)d\alpha$$

$$=K^\pm(J_a^\pm+J_b^\pm)\,,$$

where we have split the integral of $H^\pm$ over α into its contributions from the upper state ($J_a^\pm$) and from the lower state ($J_b^\pm$) and where

$$K^{\pm} = -(\sqrt{\pi}/ku)\Omega^{\pm}(\Omega^{\mp})^2 T_{tr}^2 g_{\pm}\,.$$

The parameter $T_{tr} \equiv 1/u\sqrt{D}$ plays the role of an effective transit time. This integral was evaluated for a given $\omega - \omega_0$ by fitting $H(\alpha)$ with a cubic spline and integrating the resulting expression analytically.

In this way we obtain a final line shape similar to those shown in Fig. 2. These line shapes are close to Lorentzian for large values of the parameter $\eta \equiv \gamma T_{tr}$ but as this parameter decreases below unity the line shape tends toward sharper peaking at the line center because of the increasing relative contribution of slow molecules that we have just mentioned. In the limit of zero relaxation ($\gamma_a = \gamma_b = \gamma_{ab} \to 0$) the line shape expression diverges at line center. The higher-order terms omitted in our third-order theory would describe the saturation which physically limits the amplitude of the absorbers' response. Naturally, smaller laser fields are implied by small relaxation rates, to validate our low intensity assumption.

We have plotted in Fig. 3 the resonance linewidth (half-width at half-maximum) in units of the average transit time T_{tr}. For this figure we have chosen the particular case of matched beams taken at their waist, and hence $w_{\pm} = w_0$, $L^{\pm} = 1$, and $T_{tr} = w_0/u$. Furthermore, we have assumed a common value η for the three parameters $\eta_a = \gamma_a T_{tr}$, $\eta_b = \gamma_b T_{tr}$, and $\eta_{ab} = \gamma_{ab} T_{tr}$. A curve equivalent to Fig. 3 could be plotted using γ, rather than T_{tr}, as the fixed scaling unit for the width.

We observe that this curve has three interesting

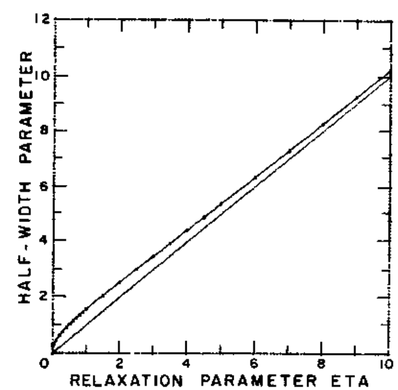

FIG. 3. Linewidth vs relaxation parameter. The linewidth (half-width at half-maximum) and relaxation rate are in units of T_{tr}^{-1}. The calculation is for matched TEM_{00} beams at their waist.

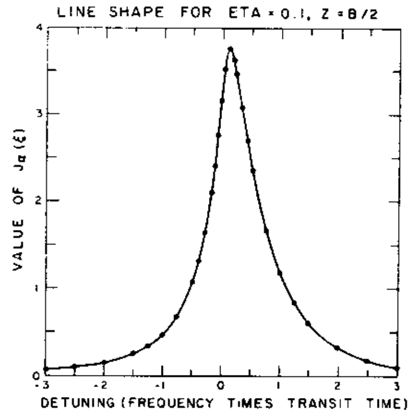

FIG. 4. Line shape for curved wave fronts. Calculated profile is for two matched beams at $z = \frac{1}{2}b$. The probe beam is diverging.

domains. At the highest pressures, the half-width tends to γ according to the law

$$\Delta\xi \equiv T_{tr}\,\Delta\omega = \eta + (2.5/\eta)\,,$$

where we have introduced the notation $\xi \equiv (\omega - \omega_0)T_{tr}$. This law and a corresponding one for small η will be derived in Sec. VII. Similar laws were recently reported by Baklanov and Chebotaev and colleagues.[36] For small values of η the line is anomalously narrow as described above, with the dependence in this case of $\Delta\xi = 1.51\sqrt{\eta}$. The strong-field theory shows the compensation of the narrowing by increased saturation.

The intermediate-broadening region is well described by the inflection tangent equation, $\Delta\xi = 0.66 + 0.94\eta$. We can compare the intercept of this tangent with the experimental value of the contribution of the transit-time broadening extrapolated to zero pressure and zero intensity in the case of the 3-μm methane line. The published experimental intercept value[24,37] $\Delta\xi/2\pi$ is $\frac{1}{8}$, whereas the theory gives a number close to 1/9.5. We regard this agreement as reasonably good since any content of higher order modes in the laser beam will increase the intercept value.

To illustrate the asymmetry in the case of a spherical wave front, Fig. 4 shows a line shape for $L^{+} = L^{-*} = 1/(1-i)$ (at $z = \frac{1}{2}b$) and $\eta = \gamma w_0/u = 0.1$. We see that the primary manifestation of asymmetry is a shift in the line that can be significant in comparison with the linewidth. This predicted asymmetry[31] was verified experimentally[38] with the usual methane line. A detailed comparison between the theory and the observations will be

given elsewhere. This shift originates in the cumulative effect of the transport of the populations across the light beam described above. In the language of hole burning we can say that the population hole created at a given point is carried across the laser beam by the molecular motion and is thus probed at an altered space-time point. If we assume, for example, that the saturating beam is diverging, we find that the sum of the Doppler shifts of the saturation beam and probe beam at a later time is always toward the blue. The system of equations comprised of $\omega + \delta = \omega_0 + kv_s$ for the saturation beam and $\omega + \delta' = \omega_0 - kv_s$ for the probe beam has the solution $\omega = \omega_0 - \frac{1}{2}(\delta + \delta')$, where $\delta + \delta'$ is always positive. Consequently the line center is red shifted.

In a more correct description the third-order process is regarded as the successive interaction of the molecule with four waves (see Appendix A). Assuming the condition for matched beams $L^{\pm} \equiv L^{\mp *}$, we have

$$\mathrm{Im}(L^{\pm}/w_{\pm}^2) = \pm k/2R\,.$$

From Eq. (77) we can calculate the total phase shift,

$$\Phi^{\pm} = -(k/2R)[\pm x_1^2 \mp (x_1 - v_r\tau)^2 \mp (x_1 - v_r\tau' - v_r\tau)^2 \pm (x_1 - v_r\tau' - 2v_r\tau)^2] - 2(\omega_0 - \omega)\tau$$

$$= \mp(kv_r^2/R)\tau(\tau + \tau') - 2(\omega_0 - \omega)\tau\,, \qquad (82)$$

where $\tau(\tau + \tau')$ is always positive.

For a diverging saturating beam (U_0^+ with $R > 0$) and a converging probe beam (U_0^-) the phase shift is

$$\Phi^- = -2(\omega_0 - \omega)\tau + (kv_r^2/R)\tau(\tau + \tau')\,.$$

In this case ω_0 is reduced and the line center is red shifted. For a converging saturating beam (U_0^-) the shift is, of course, reversed.

It is useful to know the pressure dependence of the asymmetry induced by the wave-front curvature. As an illustration, Fig. 5 shows the frequency shift of the maximum of the nonlinear resonance peak for the case $z = \frac{1}{2}b$. For high relaxation rates the atomic coherence decays before much curvature-induced phase shift is evident to

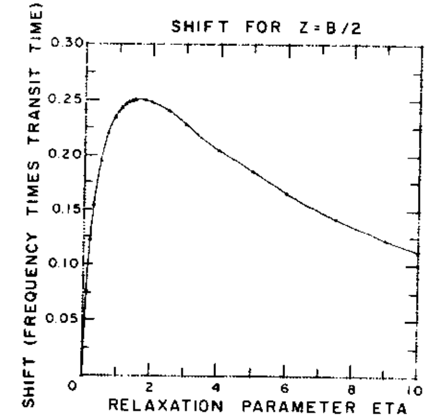

FIG. 5. Shift of the line-shape maximum as a function of the relaxation parameter. The shift and the reciprocal lifetime are in units of inverse average transit time (u/w_0). The curve is for matched beams at the position $z = \frac{1}{2}b$.

the absorber. For very weak relaxation the slow-atom contribution at zero detuning diverges so the frequency shift of the maximum again approaches zero.

VII. LINE SHAPE AFTER TRANSVERSE VELOCITY INTEGRATION

If information about transverse velocity contributions is not needed, it is attractive to reverse the order of integration in Eq. (78). The result can then be stated in the form of a single integration over the variable τ. Anticipating interest in the second-order Doppler shift, we replace ω_0 in Eq. (78) by its shifted value $\omega_0[1 - (v_r^2/2c^2)]$.

In the previous approach we also had the possibility of allowing any dependence of the γ's upon v_r. Here the first nonzero correction, a dependence of the γ's on v_r^2, could be treated in a manner parallel to the present treatment of the second-order Doppler effect. After the v_r integration we have

$$\Delta\tilde{Q}^{(3)\pm} = -\frac{2\sqrt{\pi}}{ku}\Omega^{\pm}(\Omega^{\mp})^2 g_{\pm}$$

$$\times\ \mathrm{Re}\int_0^\infty d\tau \int_0^\infty d\tau'\, \frac{e^{-\gamma_a\tau'}\exp\{-2[i(\omega_0 - \omega) + \gamma_{ab}]\tau\}}{1 + Au^2\tau'^2 + 2B_{\pm}u^2\tau\tau' + C_{\pm}u^2\tau^2 - i\omega_0(u^2/c^2)\tau}$$

$$+\ (\text{same quantity with } \gamma_a \text{ replaced by } \gamma_b)\,. \qquad (83)$$

If we introduce the variables

$$Z_1(\tau)\equiv\gamma_a\frac{B_\pm\tau}{A}+\frac{i\gamma_\pm}{u\sqrt{A}}\left(1+Du^2\tau^2-i\omega_0\frac{u^2}{c^2}\tau\right)^{1/2}$$

$$=X+iY,$$

$$Z_2(\tau)=X-iY,$$

then integration over τ' yields

$$\Delta\overline{Q}^{(3)\pm}=-\frac{\sqrt{\pi}}{ku}\Omega^*(\Omega^*)^2g_\pm\frac{1}{u^2D}\gamma_a\frac{D}{A}$$

$$\times\mathrm{Im}\int_0^\infty d\tau\,\frac{e^{Z_2}E_1(Z_2)-e^{Z_1}E_1(Z_1)}{Y}$$

$$\times\exp\{-2[i(\omega_0-\omega)+\gamma_{ab}]\tau\}$$

$$+(\text{corresponding term with }\gamma_a\text{ replaced by }\gamma_b).\tag{84}$$

For later use we will write $\Delta\overline{Q}^{(3)\pm}$ in the form

$$\Delta\overline{Q}^{(3)\pm}=K^\pm(J_a^\pm+J_b^\pm),\tag{85}$$

where $K^\pm$ was defined previously.

In Eq. (84) we recognize the imaginary part of the Fourier transform of a causal signal. Both the real and imaginary parts of such a Fourier transform are known to be Hilbert transforms. Thus the saturated absorption/saturated dispersion signals satisfy the Kramers-Kronig relations for the third-order theory in the limit of infinite Doppler width. In the plane-wave limit, Eq. (84) gives

$$\Delta\overline{Q}^{(3)\pm}=-\frac{2\sqrt{\pi}}{ku}\Omega^*(\Omega^*)^2\left(\frac{1}{\gamma_a}+\frac{1}{\gamma_b}\right)g_\pm$$

$$\times\mathrm{Re}\int_0^\infty d\tau\,\frac{\exp\{-2[i(\omega_0-\omega)+\gamma_{ab}]\tau\}}{1-i(\omega_0u^2\tau/c^2)}$$

$$=\frac{\sqrt{\pi}}{ku}\frac{\Omega^*(\Omega^*)^2}{\Delta\omega_R}\left(\frac{1}{\gamma_a}+\frac{1}{\gamma_b}\right)$$

$$\times g_\pm\,\mathrm{Im}\Big[\exp[(\omega-\omega_0+i\gamma_{ab})/\Delta\omega_R]$$

$$\times E_1\left(\frac{1}{\Delta\omega_R}(\omega-\omega_0+i\gamma_{ab})\right)\Big],$$

with $\Delta\omega_R=\omega_0u^2/2c^2$. This result was obtained previously by direct convolution of a shifted Lorentzian with the transverse velocity distribution.[39]

To compute the integrals J_α several methods have been used. The first is a direct numerical integration. This can be done either for J_α as expressed in (84), or for the equivalent integrals obtained by performing first the integration on τ in (83),

$$J_a^\pm=\mathrm{Im}\int_0^\infty d\tau'\,\frac{e^{\gamma_a\tau'}}{u\sqrt{C_\pm}Y'}[e^{Z_2'}E_1(Z_2')-e^{Z_1'}E_1(Z_1')],\tag{86}$$

with

$$Z_1'=(2/u\sqrt{C_\pm})[\gamma_{ab}+i(\omega_0-\omega)](X'+iY'),$$

$$Z_2'=(2/u\sqrt{C_\pm})[\gamma_{ab}+i(\omega_0-\omega)](X'-iY'),$$

$$X'=u(B_\pm/\sqrt{C_\pm})\tau'-i(\Delta\omega_R/u\sqrt{C_\pm}),$$

$$Y'=\{1+Au^2\tau'^2-[(B_\pm u/\sqrt{C_\pm})\tau'-i(\Delta\omega_R/u\sqrt{C_\pm})]^2\}^{1/2}.$$

The second method for calculating J_α makes use of an analytical approximation for $E_1(z)$. This is possible either when the finite lifetime is dominant or when the finite transit time is dominant.

In the first case $\gamma_\alpha/u\sqrt{A}>1$. Then the modulus of Z_1 and Z_2 will always be greater than 1 and we can make use of the asymptotic expansion for E_1[32,33]

$$E_1(z)=e^{-z}\left(\frac{1}{z}-\frac{1!}{z^2}+\frac{2!}{z^3}-\frac{3!}{z^4}+\cdots\right),$$

or better,

$$E_1(z)$$

$$=\frac{e^{-z}}{z+1}\left(1+\frac{1}{(z+1)^2}+\frac{1-2z}{(z+1)^4}+\frac{6z^2-8z+1}{(z+1)^6}+\cdots\right).$$

Still better is the Laguerre quadrature[32,40] for $E_1(z)$, which gives

$$e^zE_1(z)=\sum_{j=1}^n\frac{\lambda_j}{z+x_j},$$

where the x_j are the zeros of the Laguerre polynomials and the λ_j are the corresponding weight factors. This formula includes the first terms of the previous asymptotic expansions as the special cases

$$n=1,\ \lambda_1=1,\ x_j=0\text{ or }1.$$

Performing the integration on τ we find

$$J_a^\pm=\frac{2}{\gamma_a}\mathrm{Re}\frac{D}{C_\pm}$$

$$\times\sum_j\frac{\lambda_j}{\beta''_{\alpha j}-\beta'_{\alpha j}}[e^{\theta'_{\alpha j}}E_1(\theta'_{\alpha j})-e^{\theta''_{\alpha j}}E_1(\theta''_{\alpha j})],\tag{87}$$

where

$$\left\{\begin{matrix}\beta'_{\alpha j}\\ \beta''_{\alpha j}\end{matrix}\right\}=\frac{1}{\gamma_\alpha}\frac{B_\pm}{C_\pm}x_j-i\frac{\Delta\omega_R}{u^2C_\pm}$$

$$\mp\left[\left(\frac{1}{\gamma_\alpha}\frac{B_\pm}{C_\pm}x_j-i\frac{\Delta\omega_R}{u^2C_\pm}\right)^2-\frac{1}{u^2C_\pm}\left(1+\frac{Au^2}{\gamma_\alpha^2}x_j^2\right)\right]^{1/2}$$

and

$$\left\{\begin{matrix}\theta'_{\alpha j}\\ \theta''_{\alpha j}\end{matrix}\right\}=2[i(\omega_0-\omega)+\gamma_{ab}]\left\{\begin{matrix}\beta'_{\alpha j}\\ \beta''_{\alpha j}\end{matrix}\right\}.$$

Again, as an illustration we consider the case of matched beams, $L^\pm=L^{*\pm}=L$ and $C_\pm=2B_\pm=2LD$, $A=D\,\mathrm{Re}L$. Leaving out, for simplicity, the second-order Doppler shift we have the formula

$$J_\alpha^\pm=\sum_{j=1}^n\lambda_j\frac{1}{(\mathrm{Re}L)^{1/2}}\mathrm{Im}\left(\frac{1}{[(2L/\mathrm{Re}L)\eta_\alpha^2+x_j^2]^{1/2}}\right)$$

$$\times[e^{\theta'_{\alpha j}}E_1(\theta'_{\alpha j})-e^{\theta''_{\alpha j}}E_1(\theta''_{\alpha j})],\tag{88}$$

with

$$\left\{\begin{matrix}\theta'_{\alpha j}\\ \theta''_{\alpha j}\end{matrix}\right\}=\left[x_j\mp i\frac{(\mathrm{Re}L)^{1/2}}{L}\left(\frac{2L}{\mathrm{Re}L}\eta_\alpha^2+x_j^2\right)^{1/2}\right]$$

$$\times\left(\frac{\eta_{ab}}{\eta_\alpha}-i\frac{\xi}{\eta_\alpha}\right),$$

where

$$\eta_\alpha=\frac{\gamma_\alpha}{u\sqrt{D}},\quad\eta_{ab}=\frac{\gamma_{ab}}{u\sqrt{D}},\quad\xi=\frac{\omega-\omega_0}{u\sqrt{D}}.$$

High accuracy is obtained with $n=3$. Although the relative error is of the order of 1% for $\gamma_\alpha/u\sqrt{A}=1$ it decreases very quickly as γ_α increases. For the $n=3$ case

$$\lambda_1=0.711\,093,\quad x_1=0.415\,775$$

$$\lambda_2=0.278\,518,\quad x_2=2.294\,28$$

$$\lambda_3=0.010\,389,\quad x_3=6.29.$$

If $\gamma_\alpha/u\sqrt{A}\gg1$, it is possible to use the Laguerre quadrature formula again, this time for $e^{\theta_{\alpha j}}E_1(\theta_{\alpha j})$ in (87):

$$J_\alpha^\pm=\frac{2}{\gamma_\alpha}\mathrm{Re}\frac{D}{C_\pm}\sum_{j=1}^n\frac{\lambda_j}{\beta''_{\alpha j}-\beta'_{\alpha j}}$$

$$\times\sum_{l=1}^m\lambda_l\left(\frac{1}{\theta'_{\alpha j}+x_l}-\frac{1}{\theta''_{\alpha j}+x_l}\right).\tag{89}$$

We observe that in this approximation, the line shape is the sum of complex Lorentzians. We can use this formula, with $\sum_j\lambda_j=\sum_j\lambda_jx_j=\frac{1}{2}\sum_j\lambda_jx_j^2=1$, to obtain the first-order corrections to the plane-wave theory owing to the geometrical effects and to the second-order Doppler effect. After expansion one finds

$$J_a^\pm T_{tr}^2=\frac{1}{\gamma_a}\left(1-2\frac{Au^2}{\gamma_a^2}\right)\mathrm{Re}\left(\frac{1}{\gamma_{ab}+i(\omega_0-\omega)}\right)$$

$$-\frac{1}{\gamma_a^2}\mathrm{Re}\left(B_\pm u^2\frac{1}{[\gamma_{ab}+i(\omega_0-\omega)]^2}\right)$$

$$-\frac{1}{2\gamma_a}\mathrm{Re}\left[C_\pm u^2\frac{1}{[\gamma_{ab}+i(\omega_0-\omega)]^3}\right]$$

$$+\frac{1}{\gamma_a}\mathrm{Re}\left[i\Delta\omega_R\frac{1}{[\gamma_{ab}+i(\omega_0-\omega)]^2}\right],\tag{90}$$

where the second and third terms represent a broadening and a blue or red shift according to whether $\mathrm{Im}B_\pm$ and $\mathrm{Im}C_\pm$ are positive or negative. The second-order Doppler red shift is represented by the last term. An interesting feature of this formula is that A, $B_\pm$, and $C_\pm$ are simple functions of z, so that the integration over a finite length of absorbing material can be easily performed. To avoid cumbersome expressions we shall perform this integration only for matched beams, in which case

$$A=\frac{1}{w^2(z)}=\frac{1}{w_0^2}\frac{1}{1+4z^2/b^2},\quad C_\pm=2B_\pm=\frac{2}{w_0^2}\frac{1\pm2iz/b}{1+4z^2/b^2}.$$

We find

$$\int_{z_1}^{z_2}gJ_\alpha^\pm dz=\frac{b}{4}\left(\arctan\frac{2z_2}{b}-\arctan\frac{2z_1}{b}\right)\frac{1}{\eta_\alpha}\mathrm{Re}\left(\frac{1}{\eta_{ab}+i\xi}-i\frac{\Delta\omega_RT_{tr}}{(\eta_{ab}+i\xi)^2}\right)$$

$$-\frac{b}{8}\left[\arctan\frac{2z_2}{b}-\arctan\frac{2z_1}{b}+2b\frac{(z_2-z_1)(b^2-4z_1z_2)}{(b^2+4z_1^2)(b^2+4z_2^2)}\right]\frac{1}{\eta_\alpha}\mathrm{Re}\left[\frac{1}{\eta_\alpha^2}\frac{2}{\eta_{ab}+i\xi}+\frac{1}{\eta_\alpha}\frac{1}{(\eta_{ab}+i\xi)^2}+\frac{1}{(\eta_{ab}+i\xi)^3}\right]$$

$$\mp\frac{b^3}{2}\frac{z_2^2-z_1^2}{(b^2+4z_2^2)(b^2+4z_1^2)}\frac{1}{\eta_\alpha}\mathrm{Im}\left[\frac{1}{\eta_\alpha}\frac{1}{(\eta_{ab}+i\xi)^2}+\frac{1}{(\eta_{ab}+i\xi)^3}\right].\tag{91}$$

From these formulas we can estimate the half-width and the shift of the maximum of the resonance. In the simple case where $\eta_\alpha=\eta_{ab}=\eta$ we find that for a slice dz the half-width is

$$\Delta\xi=\eta+2.5(\mathrm{Re}L^\pm)/\eta\tag{92}$$

and the shift is

$$\delta^\pm=2.5(\mathrm{Im}L^\pm)/\eta.\tag{93}$$

For a finite length of absorbing material $(z_2 - z_1)$ the half-width is

$$\Delta\xi = \eta + 2.5K_B/\eta \qquad (94)$$

and the shift is

$$\delta^{\pm} = \pm 2.5K_S/\eta, \qquad (95)$$

where

$$K_B = \frac{1}{2} + \frac{b(z_2 - z_1)(b^2 - 4z_1 z_2)}{(b^2 + 4z_1^2)(b^2 + 4z_2^2)} \times\left(\arctan\frac{2z_2}{b} - \arctan\frac{2z_1}{b}\right)^{-1}, \qquad (96)$$

$$K_S = 2b^2\frac{z_2^2 - z_1^2}{(b^2 + 4z_1^2)(b^2 + 4z_2^2)} \times\left(\arctan\frac{2z_2}{b} - \arctan\frac{2z_1}{b}\right)^{-1}. \qquad (97)$$

In the formulas for a slice dz we observe that the broadening has an absorptionlike behavior and the shift a dispersionlike behavior versus z, both disappearing in the limit as $z \to \infty$, in which case the waves are locally plane. From the formulas for a finite cell we observe that the net shift disappears for an arrangement symmetric with respect to the waist $z_2 = -z_1$. The shift owing to the second-order Doppler effect is also easily obtained in the plane-wave limit,

$$\delta = -\Delta\omega_R = -\omega_0(u^2/2c^2). \qquad (98)$$

In addition to the Laguerre quadrature formula other rational approximations can be used for $e^z E_1(z)$. Another example is the Padé approximation,[41] which also leads to integrals that can be analytically evaluated.

The other limit is when $\gamma_\alpha/u\sqrt{A} \ll 1$, that is, when the collision and radiative relaxation processes are only a perturbation to the free-flight line shape. For this limit we may use the series representation of $E_1(z)$,

$$E_1(z) = -\Gamma - \ln z - \sum_1^{\infty}\frac{(-1)^n z^n}{n n!}, \qquad (99)$$

where Γ is Euler's constant. Each term of the series can be integrated separately, and the resulting line shape is given in Appendix C for the general case of two matched beams. In the limit of very small values of $\eta = \eta_{ab} = \eta_\alpha$ and for $z = 0$ (no curvature) this line shape has the form

$$J_\alpha = -G + \tfrac{1}{4}\pi\ln 2 - \tfrac{1}{2}\pi\Gamma - \tfrac{1}{2}\pi\ln\eta, \quad \text{for } \xi = 0, \qquad (100)$$

$$J_\alpha = G - \tfrac{1}{2}\pi(\Gamma + \ln\xi), \quad \text{for } \xi \gg \eta, \qquad (101)$$

where G is Catalan's constant and Γ Euler's constant.

The first formula shows that the free-flight line shape is logarithmically divergent at the line center. From the two preceding formulas one can deduce that the half-width is

$$\Delta\xi = \sqrt{\eta}\, 2^{-1/4} e^{3G/\pi - \Gamma/2} \simeq 1.511\sqrt{\eta}. \qquad (102)$$

This formula describes the line narrowing that occurs in the low-pressure region of Fig. 3.

Less restrictive formulas for the free-flight line shape are given in Appendix C.

VIII. EFFECTS OF FREQUENCY MODULATION AND LASER SPECTRAL WIDTH

In this section we discuss the inclusion of frequency modulation of the laser, which is required for phase-sensitive detection and which can be used as a first model for the laser spectral width. In Eq. (24) we now have a phase ϕ which is time dependent,

$$\phi = \beta\cos\omega_m t, \qquad (103)$$

with modulation frequency ω_m and modulation index β. We then express the field as the sum of discrete Fourier sidebands,

$$e^{i\omega t} e^{i\beta\cos\omega_m t} = \sum_{p=-\infty}^{\infty} i^p e^{i(\omega + p\omega_m)t} J_p(\beta), \qquad (104)$$

where the $J_p(\beta)$ are Bessel functions of integer order. At each step of the perturbation calculation we choose one of these discrete frequencies. In the third-order theory the saturated absorption signal will then appear as a quadruple sum over four sideband indices. This calculation follows the same lines as followed earlier in this paper and offer no special difficulty. Equation (78) is replaced by

$$\Delta\bar{Q}^{(3)\pm} = -\frac{2\sqrt{\pi}}{ku}\Omega^{\pm}(\Omega^{\mp})^2 g_{\pm} \times \sum_{p,q,r,s} J_s(\beta)J_r(\beta)J_q(\beta)J_p(\beta) \times \mathrm{Re}\Big(i^{s-r+q-p} e^{i(s-r+q-p)\omega_m t}\int_0^{\infty} dv_r F_2(v_r)\int_0^{\infty} d\tau \int_0^{\infty} d\tau' \exp[-v_r^2(A\tau'^2 + 2B_{\pm}\tau\tau' + C_{\pm}\tau^2)](e^{-\gamma_b\tau'} + e^{-\gamma_a\tau'}) \times \exp\{-2[i(\omega_0 - \omega) + \gamma_{ab}]\tau\} e^{i(p-q)\omega_m\tau'} e^{i(r-q+2p)\omega_m\tau}\Big), \qquad (105)$$

and in the rest of the calculation γ_α is therefore replaced by $\gamma_\alpha + i(q-p)\omega_m$ and 2ω by $2\omega + (2p + r - q)\omega_m$.

A phase-sensitive detector system will respond to one harmonic frequency in the final signal, thus imposing one condition between the four sideband indices. We note that this approach would also provide a first way to handle the problem of laser frequency noise, typically stemming from acoustic modulation of the laser structure.

In the limit of modulation slow compared with all relevant time scales for the molecules (relaxation time, transit time, etc.) this Fourier method becomes awkward owing to the large number of important sidebands. In this limit we essentially have a definite static line shape which is slowly explored by the modulation wave form. We may follow the modulation analysis method introduced by Arndt.[42] If $g(\tau)$ is the complex Fourier transform of the spectral line-shape function, then the signal at the nth harmonic of the modulation frequency is given by

$$S_n(\omega) = \mathrm{Re}\, i^n \epsilon_n \int_0^{\infty} d\tau\, g(\tau) e^{i\omega\tau} J_n(\beta\omega_m\tau), \qquad (106)$$

where $\epsilon_0 = 1$ and $\epsilon_{n\neq 0} = 2$. Since a closed-form expression for $g(\tau)$ appears in the integral of Eq. (84), we can easily obtain $S_n(\omega)$ in the general case by introducing the Bessel function $J_n(\beta\omega_m\tau)$ into the last quadrature. Finally, in the limit where effects of the finite lifetime dominate, the line shape is formed of complex Lorentzians or their derivatives. In this case, the integral in (106) can be evaluated analytically.

IX. CONCLUSIONS AND FURTHER DEVELOPMENTS

This paper appears to present the first detailed calculation of laser spectroscopy line shapes including transit-time effects. We began by noting the essential equivalence between transit-time broadening and a residual first-order Doppler effect associated with a distribution of wave vectors. The effects were considered first in their role in linear spectroscopy, such as in optical/atomic beam experiments, and a generalization of the Voigt profile [Eq. (59)] was derived for the line shape. Turning to saturation spectroscopy, we attempted to obtain a realistic approximation to the line shape, including relaxation, transit effects, and the transverse Doppler effect. Actually, we obtained, in Eq. (84), the Fourier transform of the line shape. Further approximations were introduced to obtain simpler results when either finite-lifetime or transit-time effects are dominant. The theory accounts well for experimental pressure-broadening behavior, including the residual width at low pressure owing to transit time. Further iteration between experimental and theoretical work should be pursued in order to investigate the quantitative agreement, especially in the higher-pressure domain.

Two new features appear in this theory. First, we calculate an enhanced contribution of slow molecules to the free-flight line shape, which results in a strong line-narrowing effect at very low pressures. Differential saturation and laser spectral width tend to suppress this effect. Second, we find that a dramatic shift of the center and a profile asymmetry are introduced by curvature of the laser wave fronts. The residual influence of this shift and of the transverse Doppler shift can be quantitatively estimated from the results presented here.

Let us recall the main conditions for validity of this theory, and examine possible improvements:

We have assumed a small saturation both in using a perturbation calculation and in truncating the Fourier expansions (14). A strong-field theory can be developed,[43] although more computing time is required to evaluate the line shape. The basic idea is to reduce the density matrix equations (16) to a set of coupled ordinary differential equations using the technique introduced in the discussion of the linear response. These equations can then be solved by means of a predictor-corrector numerical method. The results of such a theory agree well with the results of the present paper in the limit of small saturation parameters. The recoil effect can also be introduced into such a numerical calculation.

We have considered a pair of nondegenerate levels. This restriction can be removed for linearly polarized light when magnetic fields are absent, since we can take the quantization axis along the field polarization. All transitions then occur according to the selection rule $\Delta M = 0$, and if the sublevels are not coupled by collisions, the light interacts with independent pairs of states, so that we may simply add independent signals. An extension of this theory to three-level or even multilevel systems appears feasible.

Most of our results have calculated the line shape corresponding to a very thin slice dz of absorbing material at point z. If the gas is optically thick or if the geometry of the beam changes in an appreciable way along the absorbing cell, an additional integration over z is necessary, such as is done in Sec. VIII.

To account for recoil in the third-order theory we must first recognize that in all of our expressions for the line shape, one term (J_b) represents the probing of the hole in the lower state, whereas the other term (J_a) refers to the peak in the upper state. We may therefore simply replace the frequency ω_0 in J_b by $\omega_0[1+(\hbar\omega_0/2Mc^2)]$ and in J_a by $\omega_0[1-(\hbar\omega_0/2Mc^2)]$.

The results of this paper may serve as a first reasonable basis for the *a priori* estimation of the accuracy capability of optical frequency standards.

ACKNOWLEDGMENTS

We are happy to acknowledge the numerous stimulating conversations with our colleagues, especially with P. L. Bender. This work has been supported by the National Bureau of Standards for a number of years as part of its research program on improved precision measurement techniques for applications to basic standards. The work of one of the authors (C. V. K.) was partly supported by the National Science Foundation under Grant GP-39308X to the University of Colorado.

APPENDIX A: INTEGRAL FORM OF THE DENSITY MATRIX EQUATIONS

In the molecular frame the equation for $\rho'_{\alpha\alpha'}(\vec{r}',t',\vec{v})$ is

$$\frac{\partial\rho'_{\alpha\alpha'}}{\partial t'}=-i\omega_{\alpha\alpha'}\rho'_{\alpha\alpha'}-\gamma_{\alpha\alpha'}(\rho'_{\alpha\alpha'}-\rho'^{(0)}_{\alpha\alpha'}e^{-i\omega_{\alpha\alpha'}t'})+\frac{i}{\hbar}\sum_{\alpha''}(\rho'_{\alpha\alpha''}V'_{\alpha''\alpha'}-V'_{\alpha\alpha''}\rho'_{\alpha''\alpha'}),$$

where

$$\omega_{\alpha\alpha'}=(E_\alpha-E_{\alpha'})/\hbar \quad\text{and}\quad V'_{\alpha\alpha'}=\langle\alpha|V'(\vec{r}',t')|\alpha'\rangle.$$

Assuming that V' vanishes for $t'=-\infty$, we obtain by integration

$$\rho'_{\alpha\alpha'}(\vec{r}',t',\vec{v})-\rho'^{(0)}_{\alpha\alpha'}(\vec{r}',\vec{v})e^{-i\omega_{\alpha\alpha'}t'}$$

$$=\frac{i}{\hbar}e^{-(i\omega_{\alpha\alpha'}+\gamma_{\alpha\alpha'})t'}\int_{-\infty}^{t'}dt''e^{(i\omega_{\alpha\alpha'}+\gamma_{\alpha\alpha'})t''}\sum_{\alpha''}[\rho'_{\alpha\alpha''}(\vec{r}',t'',\vec{v})V'_{\alpha''\alpha'}(\vec{r}',t'')-V'_{\alpha\alpha''}(\vec{r}',t'')\rho'_{\alpha''\alpha'}(\vec{r}',t'',\vec{v})]$$

$$=\frac{i}{\hbar}\sum_{\alpha''}\int_0^\infty d\tau\, e^{-(i\omega_{\alpha\alpha'}+\gamma_{\alpha\alpha'})\tau}[\rho'_{\alpha\alpha''}(\vec{r}',t'-\tau,\vec{v})V'_{\alpha''\alpha'}(\vec{r}',t'-\tau)-V'_{\alpha\alpha''}(\vec{r}',t'-\tau)\rho'_{\alpha''\alpha'}(\vec{r}',t'-\tau,\vec{v})]$$

$$=\frac{i}{\hbar}\sum_{\alpha''}\int_0^\infty d\tau\, e^{-(i\omega_{\alpha\alpha'}+\gamma_{\alpha\alpha'})\tau}[\rho_{\alpha\alpha''}(\vec{r}'+\vec{v}(t'-\tau),t'-\tau,\vec{v})V_{\alpha''\alpha'}(\vec{r}'+\vec{v}(t'-\tau),t'-\tau)$$

$$-V_{\alpha\alpha''}(\vec{r}'+\vec{v}(t'-\tau),t'-\tau)\rho_{\alpha''\alpha'}(\vec{r}'+\vec{v}(t'-\tau),t'-\tau,\vec{v})].$$

From this last expression it is easy to derive the corresponding expression for $\rho_{\alpha\alpha'}(\vec{r},t,\vec{v})$ in the laboratory frame,

$$\rho_{\alpha\alpha'}(\vec{r},t,\vec{v})-\rho^{(0)}_{\alpha\alpha'}(\vec{r},\vec{v})e^{-i\omega_{\alpha\alpha'}t}=\frac{i}{\hbar}\sum_{\alpha''}\int_0^\infty d\tau\, e^{-(i\omega_{\alpha\alpha'}+\gamma_{\alpha\alpha'})\tau}[\rho_{\alpha\alpha''}(\vec{r}-\vec{v}\tau,t-\tau,\vec{v})V_{\alpha''\alpha'}(\vec{r}-\vec{v}\tau,t-\tau)$$

$$-V_{\alpha\alpha''}(\vec{r}-v\tau,t-\tau)\rho_{\alpha''\alpha'}(\vec{r}-\vec{v}\tau,t-\tau,\vec{v})].\tag{A1}$$

For each term in this sum we can draw an elementary corresponding diagram (see Fig. 6). Thus the density matrix element $\rho_{\alpha\alpha'}$ at the space-time point $(\vec{r},t)$ appears as a sum of contributions owing to interactions at previous space-time points $(\vec{r}-\vec{v}\tau,t-\tau)$ multiplied by a propagation factor describing the free precession and the decay.

When applied to the two-level system the previous equations give the optical coherence and the populations as solutions of the following integral equations:

In the molecular frame,

$$\rho'_{ab}(\vec{r}',t',\vec{v})=(n'^{(0)}_a-n'^{(0)}_b)\int_0^\infty d\tau\frac{\mu}{i\hbar}\mathcal{E}(\vec{r}'+\vec{v}(t'-\tau),t'-\tau)e^{-(i\omega_0+\gamma_{ab})\tau}$$

$$+\int_0^\infty d\tau'\frac{\mu}{i\hbar}\mathcal{E}(\vec{r}'+\vec{v}(t'-\tau'),t'-\tau')e^{-(i\omega_0+\gamma_{ab})\tau'}\int_0^\infty d\tau\frac{\mu}{i\hbar}\mathcal{E}(\vec{r}'+\vec{v}(t'-\tau'-\tau),t'-\tau'-\tau)$$

$$\times[\rho'_{ab}(\vec{r}',t'-\tau'-\tau,\vec{v})-\rho'^{*}_{ab}(\vec{r}',t'-\tau'-\tau,\vec{v})]$$

$$\times(e^{-\gamma_a\tau}+e^{-\gamma_b\tau})$$

and

$$n'_\alpha(\vec{r}',t',\vec{v})=n'^{(0)}_\alpha+\epsilon_\alpha\int_0^\infty d\tau\frac{\mu}{i\hbar}\mathcal{E}(\vec{r}'+\vec{v}(t'-\tau),t'-\tau)e^{-\gamma_\alpha\tau}\left(\int_0^\infty d\tau'\frac{\mu}{i\hbar}\mathcal{E}(\vec{r}'+\vec{v}(t'-\tau'-\tau),t'-\tau'-\tau)\right.$$

$$\times[n'_a(\vec{r}',t'-\tau'-\tau,\vec{v})-n'_b(\vec{r}',t'-\tau'-\tau,\vec{v})]$$

$$\left.\times e^{-(i\omega_0+\gamma_{ab})\tau'}-\text{c.c.}\right),$$

where $\epsilon_a=+1$ and $\epsilon_b=-1$, and where we have used the functional form of the field defined in the laboratory frame.

In the laboratory frame

$$\rho_{ab}(\vec{r},t,\vec{v})=(n^{(0)}_a-n^{(0)}_b)\int_0^\infty d\tau\frac{\mu}{i\hbar}\mathcal{E}(\vec{r}-\vec{v}\tau,t-\tau)e^{-(i\omega_0+\gamma_{ab})\tau}$$

$$+\int_0^\infty d\tau\frac{\mu}{i\hbar}\mathcal{E}(\vec{r}-\vec{v}\tau,t-\tau)e^{-(i\omega_0+\gamma_{ab})\tau}\int_0^\infty d\tau'\frac{\mu}{i\hbar}\mathcal{E}(\vec{r}-\vec{v}\tau-\vec{v}\tau',t-\tau-\tau')$$

$$\times[\rho_{ab}(\vec{r}-\vec{v}\tau-\vec{v}\tau',t-\tau-\tau',\vec{v})-\rho^*_{ab}(\vec{r}-\vec{v}\tau-\vec{v}\tau',t-\tau-\tau',\vec{v})]$$

$$\times(e^{-\gamma_a\tau'}+e^{-\gamma_b\tau'})\tag{A2a}$$

and

$$n_\alpha(\vec{r},t,\vec{v})=n^{(0)}_\alpha+\epsilon_\alpha\int_0^\infty d\tau\frac{\mu}{i\hbar}\mathcal{E}(\vec{r}-\vec{v}\tau,t-\tau)e^{-\gamma_\alpha\tau}\left(\int_0^\infty d\tau'\frac{\mu}{i\hbar}\mathcal{E}(\vec{r}-\vec{v}\tau-\vec{v}\tau',t-\tau-\tau')\right.$$

$$\times[n_a(\vec{r}-\vec{v}\tau-\vec{v}\tau',t-\tau-\tau')-n_b(\vec{r}-\vec{v}\tau-\vec{v}\tau',t-\tau-\tau')]$$

$$\left.\times e^{-(i\omega_0+\gamma_{ab})\tau'}-\text{c.c.}\right).\tag{A2b}$$

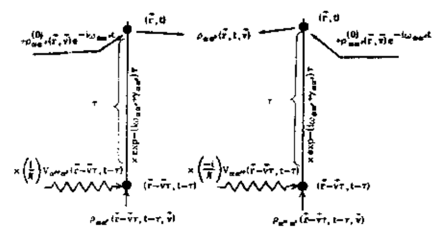

FIG. 6. Diagramatic representation of Eq. (A1). The density matrix element $\rho_{\alpha\alpha'}(\vec{r},t,\vec{v})$ of a given velocity class is given as a sum over previous interactions, modified by precession and decay effects.

A single diagram (Fig. 7) can represent the last equations. This diagram strongly suggests a perturbation approach. It is complete for the third-order calculation that we perform.

APPENDIX B. GAUSSIAN LASER MODES AND THEIR FOURIER TRANSFORMS

The laser modes are easily visualized in ordinary physical space, but the Doppler effect is more easily described in the space of wave vectors. Here we develop useful expressions in both domains for the electric field distribution of the linearly polarized laser. If $U(\vec{r})$ is the field distribution in physical space, then we shall define $U(\vec{k})$ by

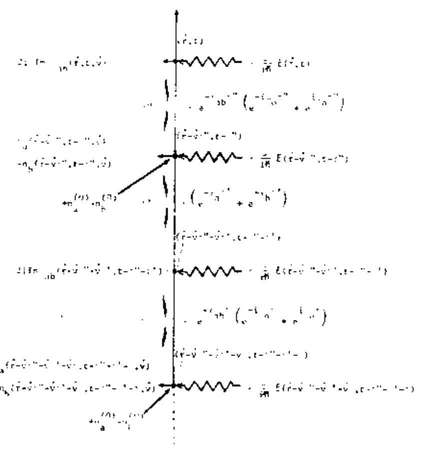

FIG. 7. Diagram representing saturated absorption. The nonlinear polarization $\rho_{ab}(\vec{r}, t, \vec{v})$ of Eq. (A2) is given by the sum over previous interaction, precession, and decay processes. The diagram is complete to third order, consistent with the general presentation of this paper; extension to higher interaction order is indicated.

$$U(\vec{r}) = \int U(\vec{k})\delta\left[\left(|\vec{k}|^2 - \frac{\omega^2}{c^2}\right)^{1/2}\right]e^{i\vec{k}\cdot\vec{r}}d^3k,$$

where the Dirac distribution in the Fourier transform of $U(\vec{r})$ insures that each plane-wave component satisfies the propagation equation

$$k_x^2 + k_y^2 + k_z^2 = \omega^2/c^2 = k^2.$$

After integration on k_z, $U(\vec{r})$ can be written as a superposition of two counterpropagating solutions

$$U^{\pm}(\vec{r}) = \int\int U^{\pm}(k_x, k_y)\exp(i\{\mp[k^2 - (k_x^2 + k_y^2)]^{1/2}(z - z_{\pm}) + k_x x + k_y y\})dk_x\, dk_y,$$

where the interpretation of the phases represented by $z_{\pm}$ will appear later. For laser beams along the z axis one can assume that k_x and k_y are much smaller than k and write

$$[k^2 - (k_x^2 + k_y^2)]^{1/2} - k - (k_x^2 + k_y^2)/2k.$$

In rectangular coordinates, we shall look for a solution with separated variables

$$U^{\pm}(\vec{r}) = \int U_x^{\pm}(k_x)\exp\left(\pm i\frac{k_x^2}{2k}(z - z_{\pm}) + ik_x x\right)dk_x \times \int U_y^{\pm}(k_y)\exp\left(\pm i\frac{k_y^2}{2k}(z - z_{\pm}) + ik_y y\right)dk_y \times e^{\mp ik(z - z_{\pm})}.$$

In both previous expressions for $U^{\pm}(\vec{r})$ we see that $U^{\pm}(k_x, k_y)$ are the Fourier transforms of the amplitude distribution $U^{\pm}(x, y, z_{\pm})$ in the $z = z_{\pm}$ planes. Thus we specify the field $U^{\pm}(\vec{r})$ everywhere by the choice of the functions $U^{\pm}(x, y, z_{\pm})$. We choose to expand these arbitrary functions in terms of the complete set of orthogonal functions formed by the products of Hermite polynomials with a Gaussian function. Since these basis functions are their own Fourier transforms, this is equivalent to the choice

$$U_x^{\pm}(k_x) = \frac{1}{\sqrt{2\pi}\Delta_{\pm}}\sum_n C_n^{\pm}H_n\left(\frac{k_x}{\Delta_{\pm}}\right)\exp\left(-\frac{k_x^2}{2\Delta_{\pm}^2}\right),$$

with a similar expression for $U_y^{\pm}(k_y)$, where $\Delta_{\pm}$ are constants, the significance of which will appear later.

Writing

$$U^{\pm}(\vec{r}) = \sum_{n,m} C_n^{\pm}C_m^{\pm}U_n^{\pm}(x, z)U_m^{\pm}(y, z)e^{\mp ik(z - z_{\pm})},$$

we get

$$U_x^{\pm}(x, z) = \frac{1}{\sqrt{2\pi}\,\Delta_{\pm}}\int_{-\infty}^{+\infty} H_n\left(\frac{k_x}{\Delta_{\pm}}\right) \times \exp\left[-\left(\frac{1}{L^{\pm}}\frac{k_x^2}{2\Delta_{\pm}^2}\right) + ik_x x\right]dk_x$$

$$= i^n(L^{\pm})^{1/2}\left(\frac{L^{\pm}}{L^{\pm *}}\right)^{n/2}e^{-L^{\pm}\Delta_{\pm}^2(x^2/2)} \times H_n[\Delta_{\pm}(L^{\pm}L^{\pm *})^{1/2}x]$$

where we have introduced the complex Lorentz function of z,

$$L^{\pm}(z) = \frac{1}{1 \mp i[\Delta_{\pm}^2(z - z_{\pm})/k]}.$$

We now make the connection between the above formalism and the usual laser mode theory.[44] The real and imaginary parts of $L^{\pm}$ can be expressed in terms of the beam radii $w_{\pm}(z)$ and of the radii of curvature of the wave fronts $R_{\pm}(z)$,

$$L^{\pm}(z) = [w_{\pm}^2/w_{\pm}^2(z)] \pm i[b_{\pm}/2R_{\pm}(z)],$$

where we have introduced the classical beam-waist radii $w_{\pm} = \sqrt{2}/\Delta_{\pm}$ and the confocal parameters $b_{\pm} = 2k/\Delta_{\pm}^2 = kw_{\pm}^2$. The amplitude of the complex Lorentz function is

$$(L^{\pm}L^{\pm *})^{1/2} = w_{\pm}/w_{\pm}(z),$$

and $(L^{\pm}/L^{\pm *})^{1/2}$ is related to the usual phase angle $\arctan(2z/b_{\pm})$ by

$$(L^{\pm}/L^{\pm *})^{1/2} = e^{\pm i\arctan 2z/b_{\pm}}.$$

The coefficients $C_n^{\pm}$, $C_m^{\pm}$, $z_{\pm}$, and $b_{\pm}$ are chosen to match the boundary conditions.

APPENDIX C: LINE SHAPE FOR LONG-LIVED SYSTEMS

We wish to calculate the integral in (84),

$$J_{\alpha}^{\pm} = \gamma_{\alpha}\frac{D}{A}\,\mathrm{Im}\int_0^{\infty} d\tau\,\frac{e^{Z_2}E_1(Z_2) - e^{Z_1}E_1(Z_1)}{Y} \times \exp\{-2[i(\omega_0 - \omega) + \gamma_{ab}]\tau\},$$

using term-by-term integration of the series

$$E_1(z) = -\Gamma - \ln z - \sum_1^{\infty}\frac{(-1)^n z^n}{nn!},$$

with

$$Z_1 = X + iY,\quad Z_2 = X - iY,$$

$$X = \gamma_{\alpha}(B_{+}/A)\tau,\quad Y = (\gamma_{\alpha}/u\sqrt{A})(1 + Du^2\tau^2)^{1/2}.$$

This procedure is justifiable when the series over which we wish to integrate is uniformly convergent on the domain $0 \le \tau < \infty$. In fact, in this Appendix we derive several conditions for convergence of the series of integrals.

For simplicity we restrict ourselves to the case of matched beams and leave out the second-order Doppler effect. In this case we have

$$L^{-*} = L^{+} = L = 1/(1 - is),\quad A/D = \mathrm{Re}L = 1/(1 + s^2),$$

$$\frac{B_{\pm}}{D} = L^{\pm} = \frac{1}{1 \mp is} = \frac{1 \pm is}{1 + s^2},$$

where $s = 2z/b$. We shall use the dimensionless variables

$$\eta_{\alpha} = \gamma_{\alpha}/u\sqrt{D},\quad \eta_{ab} = \gamma_{ab}/u\sqrt{D},$$

$$\xi = (\omega - \omega_0)/u\sqrt{D},\quad t = \tau u/\sqrt{D}.$$

X and Y are then given by

$$X = \eta_{\alpha}(1 + is)t,\quad Y = \eta_{\alpha}(1 + s^2)^{1/2}(1 + t^2)^{1/2}.$$

We note that $J_{\alpha}^{+}(\xi) = J_{\alpha}^{-}(-\xi)$, so that we need calculate only J_{α}^{+}, as given by

$$J_{\alpha}^{+} = (1 + s^2)^{1/2}\,\mathrm{Im}\int_0^{\infty} dt\,\frac{e^{X - 2(\eta_{ab} - i\xi)t}}{(1 + t^2)^{1/2}}\left[\cos Y\left(\ln\frac{X + iY}{X - iY} - \sum_{n=1}^{\infty}\frac{(-1)^n}{nn!}[(X + iY)^n - (X - iY)^n]\right) + i\sin Y\left(2\Gamma + \ln(X^2 + Y^2) + \sum_1^{\infty}\frac{(-1)^n}{nn!}[(X + iY)^n + (X - iY)^n]\right)\right].$$

To insure that the integrals in the above expression are finite we must assume $\eta_{ab} > \frac{1}{2}\eta_{\alpha}$ as a first condition. We now proceed to calculate the integral of each term in the series.

(a) The first term is

$$(J_{\alpha}^{+})_1 = (1 + s^2)^{1/2}\,\mathrm{Im}\int_0^{\infty} dt\,\frac{e^{X - 2(\eta_{ab} - i\xi)t}}{(1 + t^2)^{1/2}}\cos Y\ln\frac{X + iY}{X - iY}.$$

This is the most important term of the series; it gives the pure free-flight line shape when η_{ab} and $\eta_{\alpha} - 0$. It is also the only term that we do not know how to integrate analytically in the general case. We split the integral into two parts,

$$(J_{\alpha}^{+})_1' = (1 + s^2)^{1/2}\,\mathrm{Im}\int_0^{q} dt\,\frac{\exp[(\eta_{\alpha} - 2\eta_{ab})t + i(2\xi + s\eta_{\alpha})t]}{(1 + t^2)^{1/2}}\cos[\eta_{\alpha}(1 + s^2)^{1/2}(1 + t^2)^{1/2}]\ln\left(\frac{1 + (s + i)T}{1 - (s + i)T}\right),$$

where

$$T = [1/(1 + s^2)^{1/2}](1 + t^2)^{1/2}/t,$$

and

$$(J_{\alpha}^{+})_1'' = (1 + s^2)^{1/2}\,\mathrm{Im}\left(\{i(\tfrac{1}{2}\pi) - \ln[(1 + s^2)^{1/2} - s]\}\int_q^{\infty} dt\,\frac{\exp[\eta_{\alpha} - 2\eta_{ab})t + i(2\xi + s\eta_{\alpha})t]}{t}\cos\eta_{\alpha}(1 + s^2)^{1/2}t\right)$$

$$= \tfrac{1}{4}\pi(1 + s^2)^{1/2}\,\mathrm{Re}[E_1(q\mu^{+}) + E_1(q\mu^{-})] - \tfrac{1}{2}(1 + s^2)^{1/2}\ln[(1 + s^2)^{1/2} - s]\,\mathrm{Im}[E_1(q\mu^{+}) + E_1(q\mu^{-})],$$

where

$$\mu^{\pm} = 2\eta_{ab} - \eta_{\alpha} - i[2\xi + s\eta_{\alpha} \pm \eta_{\alpha}(1 + s^2)^{1/2}]$$

and q is an arbitrary number chosen large enough so that for $t \ge q$, one has $(1 + t^2)^{1/2}/t \simeq 1$ with the desired accuracy. (In most cases $q = 100$ is a good choice.) The first integral can be written

$$(J_\alpha^+)_\mathrm{I}' = (1+s^2)^{1/2}\int_0^q dt\, \frac{e^{(\eta_\alpha-2\eta_{ab})t}}{(1+t^2)^{1/2}}\cos[\eta_\alpha(1+s^2)^{1/2}(1+t^2)^{1/2}]\cos(2\xi+s\eta_\alpha)t\left(\pi-\arctan\frac{2t(1+t^2)^{1/2}}{(1+s^2)^{1/2}}\right)$$
$$+(1+s^2)^{1/2}\int_0^q dt\,\frac{e^{(\eta_\alpha-2\eta_{ab})t}}{(1+t^2)^{1/2}}\cos[\eta_\alpha(1+s^2)^{1/2}(1+t^2)^{1/2}]\sin(2\xi+s\eta_\alpha)t\ln\frac{\{[1-(1+s^2)T^2]^2+4T^2\}^{1/2}}{(1-sT)^2+T^2}.$$

If η_α and $\eta_{ab}\ll q^{-1}$ then this expression does not depend upon these quantities:

$$(J_\alpha^+)_\mathrm{I}' \cong (1+s^2)^{1/2}\int_0^q dt\,\frac{\cos 2\xi t}{(1+t^2)^{1/2}}\left[\pi-\arctan\left(\frac{2t(1+t^2)^{1/2}}{(1+s^2)^{1/2}}\right)\right]$$
$$+(1+s^2)^{1/2}\int_0^q dt\,\frac{\sin 2\xi t}{(1+t^2)^{1/2}}\ln\frac{\{[1-(1+s^2)T^2]^2+4T^2\}^{1/2}}{(1-sT)^2+T^2},$$

and these functions can be tabulated once and for all. If $\xi\ll q^{-1}$ also they are even independent of ξ,

$$(J_\alpha^+)_\mathrm{I}' \cong (1+s^2)^{1/2}\int_0^q dt\,\frac{1}{(1+t^2)^{1/2}}\left[\pi-\arctan\left(\frac{2t(1+t^2)^{1/2}}{(1+s^2)^{1/2}}\right)\right]$$
$$+2\xi(1+s^2)^{1/2}\int_0^q dt\,\frac{t}{(1+t^2)^{1/2}}\ln\frac{\{[1-(1+s^2)T^2]^2+4T^2\}^{1/2}}{(1-sT)^2+T^2}.$$

For $s=0$ we get

$$(J_\alpha^+)_\mathrm{I}' \cong 2\int_0^q dt\,\frac{1}{(1+t^2)^{1/2}}\arctan\left(\frac{(1+t^2)^{1/2}}{t}\right).$$

One can show that for large values of q we have

$$(J_\alpha^+)_\mathrm{I}' \cong G+\tfrac{1}{2}\pi\ln 2q,$$

where $G=0.915\,965\,594\,177\,219$ is Catalan's constant. Under the assumption that $\eta_{ab}, \eta_\alpha, \xi<q^{-1}$, we have also

$$(J_\alpha^+)_\mathrm{I}'' \cong -\tfrac{1}{4}\pi[2\Gamma+2\ln q+\tfrac{1}{2}\ln(\mu^+\mu^{+*}\mu^-\mu^{-*})],$$

so that

$$(J_\alpha^+)_\mathrm{I} \cong G-\tfrac{1}{2}\pi\Gamma+\tfrac{1}{2}\pi\ln 2-\tfrac{1}{8}\pi\ln(\mu^+\mu^{+*}\mu^-\mu^{-*}).$$

(b) The next integral we evaluate is

$$(J_\alpha^+)_\mathrm{II} = 2\Gamma(1+s^2)^{1/2}\,\mathrm{Re}\int_0^\infty dt\,\frac{e^{X-2(\eta_{ab}-i\xi)t}}{(1+t^2)^{1/2}}\sin Y$$
$$\cong 2\Gamma(1+s^2)^{1/2}\int_0^\infty e^{(\eta_\alpha-2\eta_{ab})t}\cos(2\xi+s\eta_\alpha)t\,\frac{\sin[\eta_\alpha(1+s^2)^{1/2}t]}{t}\,dt$$
$$=\Gamma(1+s^2)^{1/2}\arctan\left(\frac{2\eta_\alpha(1+s^2)^{1/2}(2\eta_{ab}-\eta_\alpha)}{(\eta_\alpha-2\eta_{ab})^2+(2\xi+s\eta_\alpha)^2-\eta_\alpha^2(1+s^2)}\right),$$

where we have approximated $\sin\eta_\alpha(1+s^2)^{1/2}(1+t^2)^{1/2}/(1+t^2)^{1/2}$ by $\sin[\eta_\alpha(1+s^2)^{1/2}t]/t$, which is valid for small η_α.

(c) For the third term we have

$$(J_\alpha^+)_\mathrm{III} = (1+s^2)^{1/2}\,\mathrm{Re}\int_0^\infty \frac{e^{X-2(\eta_{ab}-i\xi)t}}{(1+t^2)^{1/2}}(\sin Y)\ln(X^2+Y^2)\,dt$$
$$\simeq (1+s^2)^{1/2}\,\mathrm{Im}\,\eta_\alpha^2(1+s^2)\int_0^\infty e^{(\eta_\alpha-2\eta_{ab})t}\cos(2\xi+s\eta_\alpha)t\,\frac{\sin[\eta_\alpha(1+s^2)^{1/2}t]}{t}\,dt$$
$$+(1+s^2)^{1/2}\,\mathrm{Im}\int_0^\infty \frac{e^{(\eta_\alpha-2\eta_{ab})t}e^{i(2\xi+s\eta_\alpha)t}}{2t}\left(e^{i\eta_\alpha(1+s^2)^{1/2}t}-e^{-i\eta_\alpha(1+s^2)^{1/2}t}\right)\ln\left(1+2\frac{t^2}{1-is}\right)dt$$
$$\cong (1+s^2)^{1/2}\,\mathrm{Im}\,\eta_\alpha(1+s^2)^{1/2}\arctan\left(\frac{2\eta_\alpha(1+s^2)^{1/2}(2\eta_{ab}-\eta_\alpha)}{(\eta_\alpha-2\eta_{ab})^2+(2\xi+s\eta_\alpha)^2-\eta_\alpha^2(1+s^2)}\right)$$
$$+\tfrac{1}{2}(1+s^2)^{1/2}\,\mathrm{Im}[E_1(i\alpha\mu^+)E_1(-i\alpha\mu^+)-E_1(i\alpha\mu^-)E_1(-i\alpha\mu^-)],$$

where

$$\alpha=(1-is)^{1/2}/\sqrt{2}$$

where we have again assumed that η_α is small.

(d) Finally, we evaluate the remaining integrals and obtain

$$(J_\alpha^+)_\mathrm{IV}=(1+s^2)^{1/2}\sum_1^\infty\frac{(-1)^n}{nn!}(u_n+v_n),$$

where

$$u_n=\mathrm{Im}\int_0^\infty dt\,\frac{e^{X-2(\eta_{ab}-i\xi)t}}{(1+t^2)^{1/2}}\cos\{Y\}[(X+iY)^n-(X-iY)^n],$$
$$v_n=\mathrm{Re}\int_0^\infty dt\,\frac{e^{X-2(\eta_{ab}-i\xi)t}}{(1+t^2)^{1/2}}\sin\{Y\}[(X+iY)^n+(X-iY)^n].$$

Using again the approximations

$$\cos[\eta_\alpha(1+s^2)^{1/2}(1+t^2)^{1/2}]\simeq\cos[\eta_\alpha(1+s^2)^{1/2}t],$$
$$\sin[\eta_\alpha(1+s^2)^{1/2}(1+t^2)^{1/2}]/(1+t^2)^{1/2}\simeq\sin[\eta_\alpha(1+s^2)^{1/2}t]/t$$

valid for small η_α, we find

$$u_n\simeq\mathrm{Im}\,\eta_\alpha^n 2i(1+s^2)^{1/2}\times\sum_{k=0}^{(n-1)/2}(-1)^k C_n^{2k+1}(1+is)^{n-2k-1}(1+s^2)^k$$
$$\times\sum_{l=0}^k C_k^l\int_0^\infty dt\,t^{n-2(k-l)-1}e^{(\eta_\alpha-2\eta_{ab})t}\times e^{i(2\xi+s\eta_\alpha)t}\cos[\eta_\alpha(1+s^2)^{1/2}t],$$

$$v_n\simeq 2\mathrm{Re}\,\eta_\alpha^n\sum_{k=0}^{n/2}(-1)^k C_n^{2k}(1+is)^{n-2k}(1+s^2)^k$$
$$\times\sum_{l=0}^k C_k^l\int_0^\infty dt\,t^{n-2(k-l)}e^{(\eta_\alpha-2\eta_{ab})t}\times e^{i(2\xi+s\eta_\alpha)t}\times\frac{\sin[\eta_\alpha(1+s^2)^{1/2}t]}{t},$$

where the C_n^p are binomial coefficients.

After performing the integrations,

$$u_n=\mathrm{Im}\,\eta_\alpha^n 2i(1+s^2)^{1/2}\times\sum_{k=0}^{(n-1)/2}(-1)^k C_n^{2k+1}(1+is)^{n-2k-1}(1+s^2)^k$$
$$\times\sum_{l=0}^k C_k^l\frac{[n-2(k-l)-1]!}{2}\times\left(\frac{1}{(\mu^+)^{n-2(k-l)}}+\frac{1}{(\mu^-)^{n-2(k-l)}}\right),$$

$$v_n=2\,\mathrm{Re}\,\eta_\alpha^n\sum_{k=0}^{n/2}(-1)^k C_n^{2k}(1+is)^{n-2k}(1+s^2)^k$$
$$\times\sum_{l=0}^k C_k^l\frac{[n-2(k-l)-1]!}{2i}\times\left(\frac{1}{(\mu^+)^{n-2(k-l)}}-\frac{1}{(\mu^-)^{n-2(k-l)}}\right).$$

As is consistent with approximations made in the rest of the calculation, we keep only terms for which $k=l$; then

$$u_n+v_n=(n-1)!\,\eta_\alpha^n\,\mathrm{Im}\left[\left(\frac{1+is+i(1+s^2)^{1/2}}{\mu^+}\right)^n-\left(\frac{1+is-i(1+s^2)^{1/2}}{\mu^-}\right)^n\right],$$

and we have, finally,

$$(J_\alpha^+)_\mathrm{IV}=(1+s^2)^{1/2}\,\mathrm{Im}\left[F\left(\frac{1+is+i(1+s^2)^{1/2}}{\mu^+/\eta_\alpha}\right)-F\left(\frac{1+is-i(1+s^2)^{1/2}}{\mu^-/\eta_\alpha}\right)\right],$$

where F is the dilogarithm function of complex arguments, defined by

$$F(z)=\sum_{n=1}^\infty\frac{(-1)^n}{n^2}z^n.$$

This expansion will converge only if

$$|\mu^\pm|\geq\eta_\alpha\{1+[s\pm(1+s^2)^{1/2}]^2\}^{1/2}.$$

This is the final condition we require to insure convergence of the series of integrals defining J_α^+. If $\eta_{ab}=\eta_\alpha$ this requires either $\xi=0$ or

$$|\xi|\geq\tfrac{1}{2}\eta_\alpha[s+(1+s^2)^{1/2}].$$

For $\xi=0$, $\eta_{ab}=\eta_\alpha$, and $s=0$ we find

$$(J_\alpha^+)_\mathrm{IV}=-2G.$$

For $|\xi|\gg\eta_\alpha$ we can limit the calculation of F to the first few terms.

Summing the terms $(J_\alpha^+)_\mathrm{I}'$, $(J_\alpha^+)_\mathrm{I}''$, $(J_\alpha^+)_\mathrm{II}$, $(J_\alpha^+)_\mathrm{III}$, and $(J_\alpha^+)_\mathrm{IV}$ in their most general form we get a formula for J_α^+ which has an accuracy of the order of η_α^2 in a domain where the direct numerical integration of (84) is expensive. We have indeed used this formula to compute the line shape with a small table computer and obtained results which agree quite well with direct numerical integration of (84) for $\eta_{ab}, \eta_\alpha\leq 0.1$.

*Present address: Laboratoire de Physique des Lasers, Université de Paris-Nord, Saint Denis 93206, France.
†Staff Member, Laboratory Astrophysics Division, National Bureau of Standards.

[1]W. E. Lamb, Jr., in *Quantum Electronics and Coherent Light*, edited by C. H. Townes and P. A. Miles (Academic, New York, 1964), p. 78.
[2]W. E. Lamb, Jr., Phys. Rev. 134, 1429 (1964).
[3]B. J. Feldman and M. S. Feld, Phys. Rev. A 1, 1375 (1970).
[4]S. Stenholm and W. E. Lamb, Jr., Phys. Rev. 181, 618 (1969).
[5]H. K. Holt, Phys. Rev. A 2, 233 (1970).
[6]E. V. Baklanov and V. P. Chebotaev, Zh. Eksp. Teor. Fiz. 60, 552 (1971) [Sov. Phys.-JETP 33, 300 (1971)].
[7]S. Haroche and F. Hartmann, Phys. Rev. A 6, 1280 (1972).
[8]J. H. Shirley, Phys. Rev. A 8, 347 (1973).
[9]B. L. Gyorffy, M. Borenstein, and W. E. Lamb, Jr., Phys. Rev. 169, 340 (1968).
[10]S. G. Rautian, Zh. Eksp. Teor. Fiz. 51, 1176 (1966) [Sov. Phys.-JETP 24, 788 (1967)].
[11]P. R. Berman and W. E. Lamb, Jr., Phys. Rev. A 2, 2435 (1970).
[12]P. R. Berman and W. E. Lamb, Jr., Phys. Rev. A 4, 319 (1971).
[13]P. R. Berman, Phys. Rev. A 5, 927 (1972); 6, 2157 (1972).
[14]V. A. Alekseev, T. L. Andreeva, and I. I. Sobel'man, Zh. Eksp. Teor. Fiz. 62, 614 (1972) [Sov. Phys.-JETP 35, 325 (1972)]; 64, 813 (1973) [37, 413 (1973)].
[15]A. Dienes, IEEE J. Quantum Electron. QE-4, 260 (1968).
[16]A. Dienes, Phys. Rev. 174, 400 (1968).
[17]C. V. Heer and R. D. Graft, Phys. Rev. 140, A1088 (1965).
[18]M. Sargent III, W. E. Lamb, Jr., and R. L. Fork, Phys. Rev. 164, 436 (1967).
[19]M. Gorlicki, third-cycle thesis (University of Paris VI, 1975) (unpublished).
[20]M. Gorlicki and M. Dumont, C. R. Acad. Sci. B 279, 55 (1974).
[21]V. S. Letokhov, Zh. Eksp. Teor. Fiz. 56, 1748 (1969) [Sov. Phys.-JETP 29, 937 (1969)].
[22]S. G. Rautian and A. M. Shalagin, Zh. Eksp. Teor. Fiz. Pis'ma Red. 9, 686 (1969) [JETP Lett. 9, 427 (1969)]; Zh. Eksp. Teor. Fiz. 58, 962 (1970) [Sov. Phys.-JETP 31, 518 (1970)].
[23]J. L. Hall, in *Lectures in Theoretical Physics*, edited by W. E. Brittin and K. T. Mahanthappa (Gordon and Breach, New York, 1973), p. 161.
[24]C. J. Bordé and J. L. Hall, in *Laser Spectroscopy*, edited by A. Mooradian and R. G. Brewer (Plenum, New York, 1974), pp. 125–142.
[25]C. Bordé, thesis (University of Paris VI, 1972) (unpublished).
[26]B. K. Garside, IEEE J. Quantum Electron. QE-4, 940 (1968).
[27]H. Maeda and K. Shimoda, J. Appl. Phys. 46, 1235 (1975), and references therein.
[28]G. Kramer, C. O. Weiss, and J. Helmcke, Z. Naturforsch. A 30, 1128 (1975).
[29]J. L. Hall, C. Bordé, and K. Uehara, to be published; and in Proceedings of the Second Symposium on Gas Laser Physics, Novosibirsk, June 1975 (unpublished).
[30]A. P. Kol'chenko, S. G. Rautian, and R. I. Sokolovskii, Zh. Eksp. Teor. Fiz. 55, 1864 (1968) [Sov. Phys.-JETP 28, 986 (1969)].
[31]This shift was noticed first in the strong-field theory presented at the Eighth International Quantum Electronics Conference, San Francisco, 1974 (unpublished). A detailed presentation of this shift and of transit-time broadening using both the third-order theory and the strong-field theory was given in Ref. 43.
[32]M. Abramowitz and I. A. Stegun, *Handbook of Mathematical Functions* (Dover, New York, 1965).
[33]*Tables of the Exponential Integral for Complex Arguments*, Appl. Math. Ser. No. 51 (Natl. Bur. Stand., U.S. GPO, Washington, D.C., 1958).
[34]C. Bordé, C. R. Acad. Sci. Paris (to be published).
[35]J. J. Snyder and J. L. Hall, in *Proceedings of the Second Laser Spectroscopy Conference*, edited by S. Haroche (Springer, Berlin, 1975), p. 6.
[36]E. V. Baklanov and V. P. Chebotaev, in Ref. 29.
[37]J. L. Hall, in *Fundamental and Applied Laser Physics* (Esfahan Laser Symposium), edited by M. S. Feld, A. Javan, and N. Kurnit (Wiley, New York, 1973), p. 463ff.
[38]Experiments with an external methane absorption cell showed strongly asymmetric single-pass line shapes. Shifts of more than 200 kHz were observed where the linewidth was about 500 kHz.
[39]C. Bordé and F. Hartmann, unpublished.
[40]J. Todd, J. Res. Natl. Bur. Stand. (U.S.) 52, 313 (1954).
[41]Y. L. Luke, *The Special Functions and Their Approximations* (Academic, New York, 1969).
[42]R. Arndt, J. Appl. Phys. 36, 2522 (1965).
[43]C. Bordé and J. L. Hall, in Ref. 29.
[44]H. Kogelnik and T. Li, Appl. Opt. 5, 1550 (1966).

SPECTROSCOPIE. — *Forme de raie en spectroscopie à deux quanta sans élargissement Doppler.* Note (*) de M. **Christian Bordé**, présentée par **M. Alfred Kastler.**

On présente une analyse semi-classique de la forme des raies en spectroscopie à deux quanta sans élargissement Doppler qui permet de tenir compte du temps fini de traversée du faisceau par les molécules et de l'effet Doppler du deuxième ordre.

Nous nous proposons dans cette Note de présenter un profil de raie pour la spectroscopie à deux quanta sans élargissement Doppler ([1]) permettant d'inclure l'influence de la structure géométrique des faisceaux laser ainsi que celle de l'effet Doppler du deuxième ordre. Le calcul de cette forme de raie est une extension naturelle de la théorie développée pour l'absorption saturée ([2]). On considère cette fois un système de trois niveaux d'énergies $E_a < E_b < E_c$. Les molécules peuvent effectuer des transitions à deux quanta du niveau a vers le niveau c sous l'influence du champ

$$\mathscr{E}(\mathbf{r}, t) = \mathrm{Re}\left\{ E_0^+ U_0^+(\mathbf{r}) \exp[i(\omega_+ t - k_+ z + \varphi^+)] + E_0^- U_0^-(\mathbf{r}) \exp[i(\omega_- t + k_- z + \varphi^-)] \right\},$$

où les fonctions

$$U_0^\pm(\mathbf{r}) = L^\pm(z) \exp\left[-L^\pm(z) \frac{x^2+y^2}{w_\pm^2} \right]$$

traduisent la géométrie gaussienne des faisceaux et comportent des formes de Lorentz complexes $L^\pm(z)$. On se place dans l'approximation dipolaire électrique et les éléments de matrice de l'hamiltonien d'interaction sont notés : $V_{\alpha\beta} = -\mu_{\alpha\beta}\mathscr{E}$.

On suppose de plus que $V_{ac} = 0$ et que seul le niveau a est peuplé en l'absence d'irradiation. La population correspondante est écrite $n_0\, F(\mathbf{v})$ où $F(\mathbf{v})$ est la distribution normée de vitesses de Maxwell. On fera systématiquement l'approximation des ondes tournantes dans ce calcul.

La puissance absorbée par unité de longueur s'obtient pour chaque onde en projetant la polarisation électrique sur le champ correspondant :

$$\frac{\partial W_{abs}^\pm}{\partial z} = \omega_\pm E_0^\pm \,\mathrm{Im} \int dx\, dy\, d^3v\, [\mu_{bc}\rho_{cb}(\mathbf{v}) + \mu_{ab}\rho_{ba}(\mathbf{v})]\, U_0^\pm \times \exp[i(\omega_\pm t \mp k_\pm z + \varphi_\pm)] = n_0 \hbar \omega_\pm (R_{bc}^\pm + R_{ab}^\pm).$$

Les éléments non diagonaux de la matrice densité $\rho_{cb}(\mathbf{v})$ et $\rho_{ba}(\mathbf{v})$ sont calculés à l'ordre 3 à partir des équations habituelles pour la matrice densité moléculaire. On ne conserve que les termes relatifs à l'absorption à deux quanta conduisant à un élargissement Doppler réduit et à des variations lentes de $R_{bc}^\pm$ et $R_{ab}^\pm$ avec t et z. Tous ces termes possèdent la même structure et peuvent être schématisés par un diagramme. Les quatre diagrammes relatifs à l'une des deux ondes sont représentés sur la figure. Ces diagrammes présentent plusieurs perfectionnements par rapport à ceux utilisés pour l'absorption saturée ([2]). Tout d'abord